THESIS

POLYMERIC MATERIALS FOR CONTROLLED CELLULAR ADHESION AND TARGETED DELIVERY

Submitted by

Irene Lui

Department of Biochemistry and Molecular Biology

In partial fulfillment of the requirements

For the Degree of Master of Science

Colorado State University

Fort Collins, Colorado

Fall 2014

Master's Committee:

Advisor: Brian McNaughton

Santiago Di Pietro
Alan Kennan

ABSTRACT

POLYMERIC MATERIALS FOR CONTROLLED CELLULAR ADHESION AND TARGETED DELIVERY

Gaining control over cell adhesion and growth is a critical step in a variety of biomedical applications. Controlling the localization of cell adhesion and growth is typically achieved by coating a non-adhesive surface with adhesive small molecule or macromolecule reagents with affinity for a cell surface component. Cell-imprinting a hydrogel from a monolayer of cells transforms this material into a substrate for mammalian cell adhesion and growth. Cell-imprinted polyacrylamide hydrogels can be used as an inexpensive and simple substrate for directing cell adhesion and growth. Separately, as a result of a selection to identify a PC-3 prostate cancer cell-selective cell-penetrating peptide, a linear 12-amino acid peptide "Ypep" (N-YTFGLKTSFNVQ-C) has been identified, whose cell penetration potency and selectivity profiles are tightly controlled by multivalency effects. Alanine scanning mutagenesis was used to assess the specific contribution each residue plays in cell uptake efficiency and cell selectivity. The best mutant exhibits ~19-fold better uptake efficiency and ~4-fold improved cell-selectivity for a human prostate cancer cell line.

ACKNOWLEDGEMENTS

To begin, I would like to thank my advisor, Professor Brian McNaughton. His encouragement and support have meant more to me than I can properly express. I would not be the scientist I am today without him. The encouragement of my family has also been invaluable. They've always supported my love for research even during the hardest of times.

TABLE OF CONTENTS

LIST OF TABLES

Chapter 1

LIST OF FIGURES

CHAPTER ONE

CONTROLLED CELLULAR ADHESION AND TARGETED CELLULAR DELIVERY

1.1 Introduction

This thesis describes two conceptually distinct research projects: (1) The use of cell-imprinted polymers as substrates for controlled cell adhesion and growth of mammalian cells on a two-dimensional substrate; and, (2) The development of a novel protein transduction domain with uptake potency and cell-selectivity profiles that are controlled by multivalency effects. As such, this chapter is essentially divided into two halves. In part one, I describe current methods for controlling mammalian cell adhesion and growth on two-dimensional substrates, and discuss previous work on molecularly-imprinted polymers, which makes up the conceptual basis for my own work. In part two, I describe recent efforts to facilitate exogenous protein delivery to mammalian cells, including the use of protein transduction domains.

Part One

1.2 Approaches to Control Cell Adhesion and Growth

A fundamental requirement for the culture of adherent cell lines is generation of a substrate onto which the cells can grow. Additionally, many cellular assays,

studies on cell adhesion, tissue generation, cell-cell interfaces, and tissue engineering require precise arrangement of cells within a 2- or 3-dimensional matrix.[1–8] Thus, the ability to control cell adhesion and growth is central to increasing our understanding of cell migration and cellular interfaces, as well as the construction of complex cellular or multicellular arrangements.

While satisfactory for simple tissue culture, growing cells in customary polystyrene plates equipped with a polycarboxylate coating is inadequate for controlling cell motility, cell morphology, and localization.[9] Unsurprisingly, researchers have dedicated a significant amount of effort to the generation of technologies and reagents that provide control over the spatial localization of mammalian cells on a synthetic substrate. Generally, these approaches to controlling cell adhesion and growth include: (1) The development of patterned peptide reagents that bind a particular cell;[10] (2) The use of patterned single-stranded DNA (ssDNA) and complementary ssDNA cellular display;[11] and (3) patterned lipid membranes,[12] which are described below.

In each case study, potential applications of perfecting controlled growth of mammalian cells will be described in the context of utility, practicality, cost, and challenges.

1.3 Peptide Mediated Cellular Adhesion

Self-assembled monolayers (SAMs) have been previously utilized in cell attachment and patterning.[13–15] By incorporating different compounds that bind cell-surface receptors into SAMs (proteins, peptides, carbohydrates, and small molecules) specific cell types can be bound. Using a cytophobic fluorous SAM as a background, alkane thiols (ATs) with preattached peptides (RGD or YIGSR) were spotted in bare gold holes throughout the membrane (Figure 1.1).

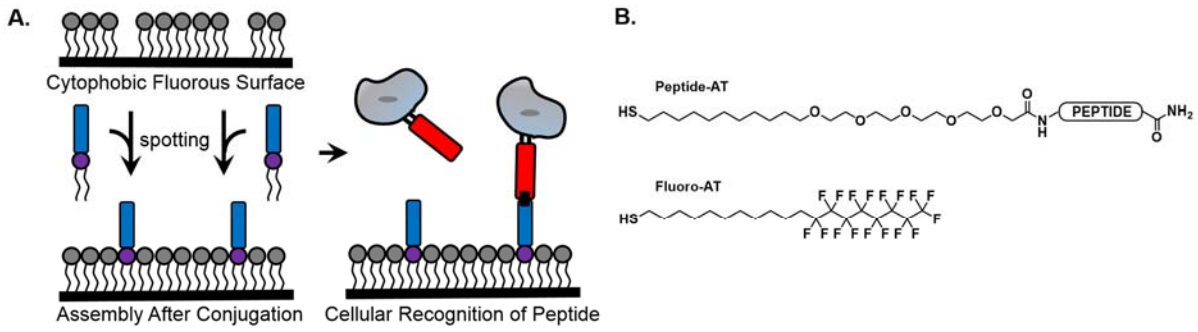

Figure 1.1 (A) Cytophobic fluorous-alkane thiols (ATs; grey) are layered on a solid substrate. Peptide-ATs (purple) spotted in holes on the monolayer act as substrates for cellular attachment. Incubating cells displaying the proper receptor allow for targeted binding. (B) Structure of peptide-AT and fluoro-AT.

These surfaces were then tested to determine if they could selectively bind their target cell lines. RGD spotted surfaces preferentially bound Swiss 3T3 fibroblasts with no adhesion from SH-SY5Y neuroblastomas. Surfaces displaying YIGSR on the other hand, had SH-SY5Ys strongly adhering with only modest adhesion by 3T3s. These results indicate the designed arrays are binding the correct target cells.[10] Production of these ligand presenting surfaces can be utilized for cell-based screens and to create arrays that further the understanding in controlling cellular growth and processes.

1.4 Programmed Cell Adhesion with Oligonucleotides

Chemical modifications are a common method of controlling cellular adhesion.[16,17] However, the irreversibility of these reactions can interfere with intracellular signaling studies. Previous modifications to cell surface proteins with DNA have had some consequences: cytoskeleton perturbation, activation of cell-surface receptors, and non-specific engagement of adhesion machinery activating intracellular signaling cascades.[18–20] Despite these side effects, there are several advantages of using DNA, including easy synthesis and modification, strong and rapid interactions, and reversibility through the use of DNase. Therefore, an alternative means of using DNA to program cellular adhesion without modification of cell surface proteins has been developed.[11]

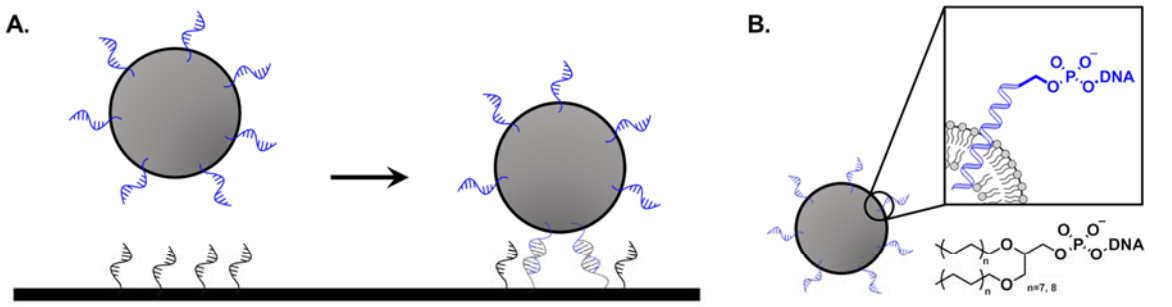

Figure 1.2 (A) Aldehyde coated glass slide modified with ssDNA template (black) is treated with a cell coated with the complementary ssDNA (blue). Single strands anneal, anchoring the cell to the surface. (B) ssDNA modified on the 5' end with dialkylphosphoglyceride incorporated in the cell membrane non-covalently.

Single stranded oligonucleotides were modified with C_{16} dialkylphosphoglyceride on the 5' end and through flow cytometry, were found to

easily incorporate into Jurkat cell membranes non-covalently and within five minutes of mixing. With the addition of polydeoxythymidine linkers between a 100mer and the lipid anchor, cells were immobilized on glass bearing complementary DNA sequences. The modified cells displayed morphology similar to unmodified cells and were still capable of cell-to-cell interaction and normal proliferation.[11] With these lipid-modified oligonucleotides, further studies on membrane mechanics, tissue engineering, and biological processes close to the cell surface can be more easily conducted.

1.5 Patterned Lipid Membranes

Different chemical and physical characteristics of surfaces can influence and control cellular adhesion and behavior.[21,22] The use of phospholipid membranes mounted on solid substrates have shown to effectively mimic cell surfaces.[23,24] Through a mix of phosphatidylcholine (PC), positively charged lipids, negatively charged phosphatidylserine (PS) in various doping ratios, cellular adhesion is promoted by 6 hours of incubation, even with mild agitation. At 24 hours, cells exhibited normal morphology. However, membranes lacking PS, even in the presence of other types of phospholipids such as phosphatidylglycerol (PG) and phosphatidylethanolamine (PE), failed to promote attachment and growth of cells.

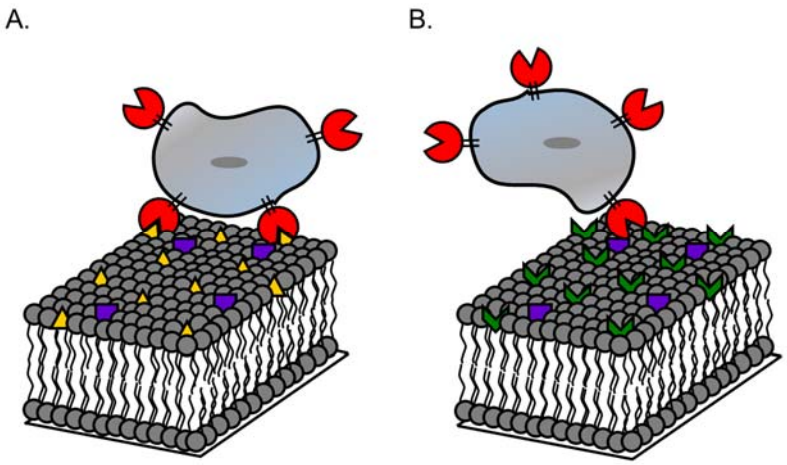

Figure 1.3 Lipid mediated cellular adhesion and patterning. A small water layer between the solid substrate and bilayer allows for lateral diffusion of lipids. (A) Solid silica coated with a lipid bilayer composed of PC (●), PS (▲), and PE (■) promotes cellular adhesion by unmodified cells. (B) Substituting PS for PG (▼) abolishes binding of cells to the artificial membrane.

These membranes also exhibited lateral fluidity, but cells remained anchored to their locations; this indicates that PS likely acts as an initial linkage point while allowing cells to deposit extracellular matrix proteins to form a permanent attachment.[12] The use of PS in fluid membranes to mediate cellular adhesion is a simple technique that allows for greater control and evolution in cell-patterning technologies.

1.6 Molecularly-Imprinted Polymers

Expanding on the previously mentioned studies, molecularly-imprinted polymers (MIPs) have been developed as various types of biomedical tools.[9,25] One type of MIP relies on the controlled design of topographical patterns that vary the texture on the surface of polymers without mixing in any of the substrates mentioned earlier. Different patterns affect the strength of cellular adhesion and rate of migration.[26,27] For other MIPs, synthetic polymers are cross-linked in the presence of a target molecule or receptor (imprint molecule). The imprint molecule is then washed away, leaving behind an impression of similar shape and size.[28] (Figure 1.4)

Such MIPs are primarily used to identify the presence of various substrates, from small molecules to macromolecules[28,29], but have also been shown to be capable of facilitating cell growth while non-imprinted gels are unable to sustain cellular growth.[12,30]

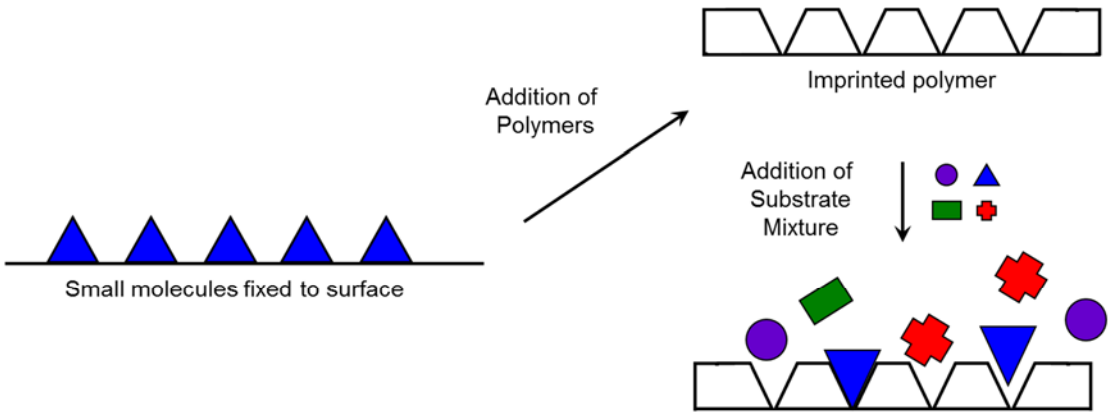

Figure 1.4 Molecularly Imprinted Polymers. Polymers are cast and cross-linked on a surface fixed with small molecules. Formed polymeric surface contains imprints of the substrate and can be used to identify the target molecule in the presence of other substrates.

Part Two

1.7 Challenges Associated with the Use of Proteins as Modulators of Cell Function and Fate

Recent studies suggest that only a small percentage (approximately 15 - 25%) of the human proteome is susceptible to modulation by traditional small molecule drugs. This is because most proteins lack well-defined small molecule binding

pockets typically found in enzymes. As a result, the functional diversity of disease-relevant proteins successfully targeted by small molecule drugs is low. Approximately 40% of all prescription drugs target a single class, the G-Protein Coupled Receptors (GPCRs), and the remaining small molecule drugs mainly target enzymes.

Even the relatively modest number of proteinaceous cellular probes and therapies (including ~200 protein drugs currently available worldwide) have demonstrated the remarkable ability of proteins as modulators of cell function and fate. The relatively large size, high folding energies (typically >7 kcal/mol), well-defined three-dimensional structure and functional group diversity (by virtue of the proteinogenic amino acids) allow proteins to bind macromolecular surfaces that can evade small molecules. In addition, identifying new proteins that bind a particular disease-relevant target may be substantially simpler than the analogous small molecule discovery. Small molecule drug discovery is a particularly arduous process, which requires chemical synthesis, purification, and relatively low throughput screening (typically ~10^4 - 10^6) that often requires expensive robotics. In contrast, screening ~10^7 - 10^{12} member protein libraries has become common practice, through the application of high-throughput tools such as phage display, yeast display, split-protein reassembly, and flow cytometry.

What then, is the primary obstacle to the broader use of proteins as drugs and basic research tools? In contrast to most small molecules, proteins typically do not cross the lipid bilayer membrane of mammalian cells. This dramatically narrows the utility of protein reagents and therapeutics to those that target cell surface receptors.

DNA, and thus the proteins they encode, can be delivered to a variety of mammalian cells using recombinant viruses. However, viral vectors can elicit strong mammalian immune system responses that can destroy the vector and harm the subject. Viral gene delivery typically results in the random insertion of therapeutic genes in the subject's genome. Since this insertion can disrupt endogenous genes associated with cell growth regulation, viral transduction can increase the risk of malignancy.[31,32] In addition, viral transduction methods can suffer from variable expression between transduced cells and a significant lag time prior to expression of therapeutic molecules.[33]

Current non-viral methods for the delivery of proteins to mammalian cells include electroporation, microinjection, cationic lipids, viral peptide fusions, and polycationic transduction domains. Like viral-dependent approaches, these methods generally have properties that limit their broad use. For example, the efficiency of protein delivery via electroporation varies greatly, and is often quite low. In addition, the electroporation of mammalian cells is highly cytotoxic, limiting its use mostly to *in vitro* cell culture experiments.[34] Microinjection physically introduces

protein directly into the cell, but requires extensive training and specialized equipment, limiting its use. In addition, limitations on the number of cells a researcher or clinician can reasonably microinject makes this method poorly suited for *in vivo* applications.[35]

Cationic lipids have been used extensively to deliver DNA and RNA to mammalian cells *ex vivo*. More recently, these reagents have been applied successfully to the delivery of proteins as well. However, unlike oligonucleotides, which universally have a high negative charge, and thus interact well with cationic lipids, the diversity protein net charge and hydrophobicity in proteins greatly influences the extent to which they interact with cationic lipids, resulting in highly variable internalization efficiencies. Moreover, many mammalian cell types are well known to resist transfection with cationic lipids.

1.8 Protein Transduction Domains / Cell-Penetrating Peptides

One attractive approach to protein delivery in mammalian cells is the use of cationic protein transduction domains (PTDs) or cell-penetrating peptides (CPPs). CPPs are polypeptides that are capable of entering cells when applied extracellularly. This method of protein delivery offers a multitude of advantages over approaches that require viral platforms. They are comparatively easy to produce, can be genetically fused to protein cargo, and are inherently transient *in*

vivo through protein degradation. CPPs achieve entry within minutes and show uniform transduction between cells in culture, and are generally not cytotoxic.[36,37] Since the discovery that exogenous HIV-TAT protein can enter cells and activate transcription,[38,39] a number of natural and synthetic CPPs have been described, including some from our lab. HIV-TAT, penetratin, and oligoarginine (such as Arg_{10}) comprise the most well-studied peptide PTDs.[40]

Published in 1988, the first known CPP was derived from the Tat protein of the human immunodeficiency virus 1 (HIV-1). When it was observed that the exogenously expressed protein was taken up by cells and activated genes in the HIV-1 viral vector, the responsible peptide domain (named Tat after the protein in which it was discovered) was further investigated. An additional peptide domain, penetratin, was derived from the Antennapedia homeodomain when it was found that externally applied protein accumulated in cells as well. Through site-directed mutagenesis, the peptide sequence necessary and sufficient for translocation was discovered, building the foundation for the study of additional CPPs.[41–43] From these initial studies, hundreds of CPPs have been derived from existing proteins or synthesized based on known models.

1.9 Structure of Cell-Penetrating Peptides

Through the study of the aforementioned and other CPPs, it has been found that these peptide domains can range anywhere from 6 to 30 amino acids in length (few being greater than 30 residues long) and are generally cationic, with a few being amphipathic.[44–46] Based on the structure of these naturally derived peptides,[47,48] synthetic CPPs, such as oligoarginine (R_9)[49] or transportan[50] have also been constructed.

Cell-penetrating peptides can be divided into two classes: those derived from domains occurring naturally in proteins (such as penetratin and Tat) and artificial synthetic (or chimeric) peptides. Within each class, there are various types of peptides, each of which can have dozens of analogs based on the parent peptide. These analogs were produced through mutations, insertions, and deletions and many function just as well, if not better than the original sequence.[47,51,52]

Table 1.1 Parent sequences of various CPPs

Name	Sequence	Reference
Naturally Derived Peptides		
Tat	GRKKRRQRRRPPQC	38, 39
Penetratin	RQIKIWFQNRRMKWKK	41-43
Nuclear Localization Sequence Based Peptides	PKKKRKV	51
pVEC	LLIILRRRIRKQAHAHSK	48
Synthetic Peptides		
Transportan	GWTLNSAGYLLKINLKALAALAKKIL	48
Amphiphilic Model Peptide	KLALKLALKALKAALKLA	44-46
Arg_9	RRRRRRRRR	47

Despite large variations in amino acid sequence, the majority of CPPs contain a high net positive charge at physiological pH.[52] Studies have shown that a CPPs ability to cross the lipid bilayer does depend on the presence of these positive charges, but the rest of the sequence plays a large role in determining relative uptake efficiency.[53] It is also important to notice that length of the peptide plays a large role in function. Even if certain domains were found to be critical in cell penetration, if they were individually isolated but were too short (<6 amino acids), their ability to enter a cell was abolished.[54]

Synthetic CPPs are constructed based on the properties of the naturally occurring peptides. As most of those discovered contained a high net positive charge, a large percentage of each synthetic peptide produced contains several arginine, lysine, and/or histidine residues. While there is some methodology to predicting the structure of CPPs, many, however, come about as a result of experiments attempting to construct peptides with entirely different functions.[55] Currently, phage display libraries on filamentous phage are commonly used to find new CPPs.[56] Libraries containing upwards of 10^{10} unique phage with displayed peptides can be screened for highly efficient penetration of mammalian cells.

1.10 Mechanism of Internalization

The mechanism of internalization by cell-penetrating peptides into cells varies from construct to construct, likely because of a lack of sequence and structural homology. However, the exact pathways for most studied CPPs are not clearly understood and have only been described in the most general terms. Some reports find that internalization of arginine rich peptides is inhibited by incubation at low temperatures and ATP depletion, indicating an energy-dependent mechanism.[57] These findings are often coupled with the hypothesis that CPPs enter through some pathway of endocytosis as the peptide can often be found in endocytic vesicles of cells.[57–60] However, there are also contradicting studies that cell penetration by the same subset of peptides still occurs at 4°C, indicating an energy independent mechanism: that internalization is receptor and endocytosis independent.[61–63] This mechanism suggests a model of direct penetration or translocation that can also occur through various pathways.[64,65] It has also been suggested that the method of internalization may be affected by the type of cargo conjugated to the CPP: larger molecules transported via energy-dependent macropinocytosis[66] while small molecule cargo leads to internalization through electrostatic interactions and hydrogen bonding.[67] Further investigations need to be conducted to acquire a more thorough understanding of how these peptides function and to determine which of the previous studies have the most valid claims.

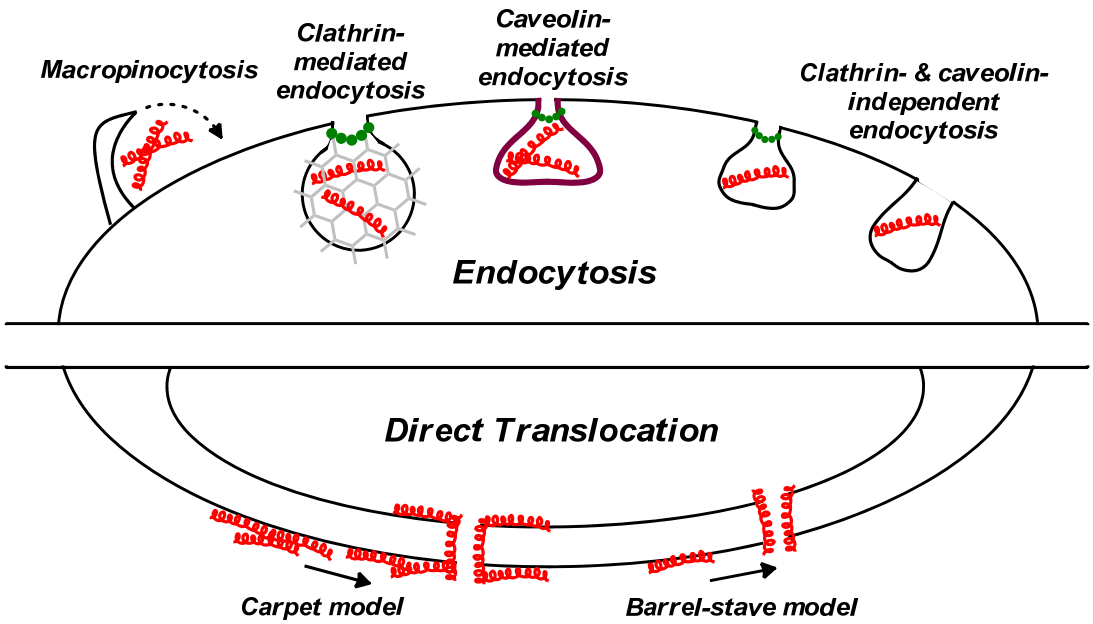

Figure 1.5 Cell-penetrating peptide entry into cells depends on sequence, structure, and possibly charge. Penetration has shown to occur through any of the known endocytic mechanisms or through the various mechanisms of direct translocation.

1.11 Current Studies and Uses of Cell-Penetrating Peptides

This class of peptides is unique in that they have the ability to cross the lipid bilayer of cells and bring attached substances with it. Many macromolecules have low biomembrane permeability and can only enter the cell if specialized, molecule-specific channels or pumps are present. As a result, many compounds with potential use as therapeutics have been discarded because of an inability to traverse the membrane.

Due to their ability to easily translocate the cellular membrane, the majority of research has been focused on fusing CPPs to cargo and studying their ability to deliver molecules of various sizes to mammalian cells *in vitro* and *in vivo*.[68] Various

other delivery vehicles have been designed to deliver large quantities of cargo: antibodies,[69] nanoparticles,[70,71] and liposomes[72] to name a few. While relatively effective, they can often elicit an immune response in the host or are immediately filtered out of the blood by the liver and spleen before they have the opportunity to interact with target tissue.[73] In addition to this, production of these delivery vehicles can be costly with a short shelf life.[74] CPPs on the other hand have low toxicity, are non-immunogenic, and can remain *in vivo* for some period of time. However, they are limited in their specificity and will often deliver cargo to any cell they interact with. In addition to this, CPPs are also susceptible to proteolytic cleavage and stand the risk of being inactivated before reaching their target.[37] Currently, various studies are being conducted to improve the specificity of these peptides for certain cell types and to develop methods to protect them from cleavage *in vivo*.[75]

REFERENCES

(1) Singhvi, R., Kumar, A., Lopez, G., Stephanopoulos, G., Wang, D., Whitesides, G., and Ingber, D. (1994) Engineering cell shape and function. *Science (80-.). 264*, 696–698.

(2) Atala, A., Bauer, S. B., Soker, S., Yoo, J. J., and Retik, A. B. (2006) Tissue-engineered autologous bladders for patients needing cystoplasty. *Lancet 367*, 1241–6.

(3) Raya-Rivera, A., Esquiliano, D. R., Yoo, J. J., Lopez-Bayghen, E., Soker, S., and Atala, A. (2011) Tissue-engineered autologous urethras for patients who need reconstruction: an observational study. *Lancet 377*, 1175–82.

(4) Ott, H. C., Matthiesen, T. S., Goh, S.-K., Black, L. D., Kren, S. M., Netoff, T. I., and Taylor, D. a. (2008) Perfusion-decellularized matrix: using nature's platform to engineer a bioartificial heart. *Nat. Med. 14*, 213–21.

(5) Hench, L. L., and Polak, J. M. (2002) Third-generation biomedical materials. *Science 295*, 1014–7.

(6) Tibbitt, M. W., and Anseth, K. S. (2009) Hydrogels as extracellular matrix mimics for 3D cell culture. *Biotechnol. Bioeng. 103*, 655–63.

(7) Chua, C. (2001) Review The Design of Scaffolds for Use in Tissue Engineering. Part I. Traditional Factors *7*, 679–689.

(8) Chua, C. (2002) Review The Design of Scaffolds for Use in Tissue Engineering. Part II. Rapid Prototyping Techniques *8*, 1–11.

(9) Lotfi, M., Nejib, M., and Naceur, M. Cell Adhesion to Biomaterials : Concept of Biocompatibility.

(10) Orner, B. P., Derda, R., Lewis, R. L., Thomson, J. a, and Kiessling, L. L. (2004) Arrays for the combinatorial exploration of cell adhesion. *J. Am. Chem. Soc. 126*, 10808–9.

(11) Selden, N. S., Todhunter, M. E., Jee, N. Y., Liu, J. S., Broaders, K. E., and Gartner, Z. J. (2012) Chemically programmed cell adhesion with membrane-anchored oligonucleotides. *J. Am. Chem. Soc. 134*, 765–8.

(12) Groves, J. T., Mahal, L. K., and Bertozzi, C. R. (2001) Control of Cell Adhesion and Growth with Micropatterned Supported Lipid Membranes 5129–5133.

(13) Faucheux, N., Schweiss, R., Lützow, K., Werner, C., and Groth, T. (2004) Self-assembled monolayers with different terminating groups as model substrates for cell adhesion studies. *Biomaterials 25*, 2721–30.

(14) Keselowsky, B. G., Collard, D. M., and García, A. J. (2003) Surface chemistry modulates fibronectin conformation and directs integrin binding and specificity to control cell adhesion. *J. Biomed. Mater. Res. A 66*, 247–59.

(15) Schreiber, F. (2000) Structure and growth of self-assembling monolayers. *Prog. Surf. Sci. 65*, 151–257.

(16) Aplin, A. E., Howe, A. K., and Juliano, R. L. (1999) Cell adhesion molecules, signal transduction and cell growth. *Curr. Opin. Cell Biol. 11*, 737–44.

(17) Lee, J. H., Jung, H. W., Kang, I. K., and Lee, H. B. (1994) Cell behaviour on polymer surfaces with different functional groups. *Biomaterials 15*, 705–11.

(18) Douglas, E. S., Chandra, R. a, Bertozzi, C. R., Mathies, R. a, and Francis, M. B. (2007) Self-assembled cellular microarrays patterned using DNA barcodes. *Lab Chip 7*, 1442–8.

(19) Hsiao, S. C., Shum, B. J., Onoe, H., Douglas, E. S., Gartner, Z. J., Mathies, R. a, Bertozzi, C. R., and Francis, M. B. (2009) Direct cell surface modification with DNA for the capture of primary cells and the investigation of myotube formation on defined patterns. *Langmuir 25*, 6985–91.

(20) Zhao, W., Loh, W., Droujinine, I. a, Teo, W., Kumar, N., Schafer, S., Cui, C. H., Zhang, L., Sarkar, D., Karnik, R., and Karp, J. M. (2011) Mimicking the inflammatory cell adhesion cascade by nucleic acid aptamer programmed cell-cell interactions. *FASEB J. 25*, 3045–56.

(21) Lim, J. Y., and Donahue, H. J. (2007) Cell sensing and response to micro- and nanostructured surfaces produced by chemical and topographic patterning. *Tissue Eng. 13*, 1879–91.

(22) Bures, P., Huang, Y., Oral, E., and Peppas, N. a. (2001) Surface modifications and molecular imprinting of polymers in medical and pharmaceutical applications. *J. Control. Release 72*, 25–33.

(23) Engler, A., Bacakova, L., Newman, C., Hategan, A., Griffin, M., and Discher, D. (2004) Substrate compliance versus ligand density in cell on gel responses. *Biophys. J. 86*, 617–28.

(24) Discher, D. E., Janmey, P., and Wang, Y.-L. (2005) Tissue cells feel and respond to the stiffness of their substrate. *Science 310*, 1139–43.

(25) Jones, F. (2001) Teeth and bones: applications of surface science to dental materials and related biomaterials. *Surf. Sci. Rep. 42*, 75–205.

(26) Clark, P., Connolly, P., Curtis, A., Dow, J., and Wilkinson, C. (1990) Topographical control of cell behaviour: II. Multiple grooved substrata. *Development 108*, 635–644.

(27) Jiang, X., Takayama, S., Qian, X., Ostuni, E., Wu, H., Bowden, N., LeDuc, P., Ingber, D. E., and Whitesides, G. M. (2002) Controlling Mammalian Cell Spreading and Cytoskeletal Arrangement with Conveniently Fabricated Continuous Wavy Features on Poly(dimethylsiloxane). *Langmuir 18*, 3273–3280.

(28) Haupt, K. (2001) Molecularly imprinted polymers in analytical chemistry. *Analyst 126*, 747–756.

(29) Ye, L., and Haupt, K. (2004) Molecularly imprinted polymers as antibody and receptor mimics for assays, sensors and drug discovery. *Anal. Bioanal. Chem. 378*, 1887–97.

(30) Kim, E. K. F., Reano, R. M., Pang, S. W., Yee, A. F., Chen, C. S., and Leong, K. W. (2005) Nanopatterned-induced changes in morphology and motility of smooth muscle cells. *Biomaterials 26*, 5405–5413.

(31) Verma, I. M., and Somia, N. (1997) Gene therapy -- promises, problems and prospects. *Nature 389*, 239–42.

(32) Nayak, S., and Herzog, R. W. (2010) Progress and prospects: immune responses to viral vectors. *Gene Ther. 17*, 295–304.

(33) Górecki, D. C. (2001) Prospects and problems of gene therapy: an update. *Expert Opin. Emerg. Drugs 6*, 187–98.

(34) Kalinski, T., Jaquet, K., Langen, R., Wang, L., Gabbert, H. E., and Gerharz, C. D. (1997) An optimized electroporation protocol for transfection of sensitive cell lines using basic laboratory equipment *11*, 717–722.

(35) Celis, J. E. (1984) Microinjection of somatic cells with micropipettes: comparison with other transfer techniques. *Biochem. J. 223*, 281–91.

(36) Veldhoen, S., Laufer, S. D., Trampe, A., and Restle, T. (2006) Cellular delivery of small interfering RNA by a non-covalently attached cell-penetrating peptide: quantitative analysis of uptake and biological effect. *Nucleic Acids Res. 34*, 6561–73.

(37) Koren, E., and Torchilin, V. P. (2012) Cell-penetrating peptides: Breaking through to the other side. *Trends Mol. Med. 18*, 385–393.

(38) Frankel, A. D., and Pabo, C. O. (1988) Cellular uptake of the tat protein from human immunodeficiency virus. *Cell 55*, 1189–1193.

(39) Green, M., and Loewenstein, P. M. (1988) Autonomous functional domains of chemically synthesized human immunodeficiency virus tat trans-activator protein. *Cell 55*, 1179–88.

(40) Milletti, F. (2012) Cell-penetrating peptides: classes, origin, and current landscape. *Drug Discov. Today 17*, 850–60.

(41) Derossi, D., and Prochiantztn, M. (1994) The Third Helix of the Antennapedia Homeodornain Translocates through Biological membranes. *J. Biol. Chem. 269*, 10444–10450.

(42) Derossi, D., Chassaing, G., and Prochiantz, A. (1998) Trojan peptides: the penetratin system for intracellular delivery. *Trends Cell Biol. 8*, 84–87.

(43) Thorén, E. G., Persson, D., Karlsson, M., and Nordén, B. (2000) The Antennapedia peptide penetratin translocates across lipid bilayers - the first direct observation. *FEBS Lett. 482*, 265–268.

(44) Oehlke, J., Scheller, A., Wiesner, B., Krause, E., Beyermann, M., Klauschenz, E., Melzig, M., and Bienert, M. (1998) Cellular uptake of an alpha-helical amphipathic

model peptide with the potential to deliver polar compounds into the cell interior non-endocytically. *Biochim. Biophys. Acta 1414*, 127–139.

(45) Wyman, T. B., Nicol, F., Zelphati, O., Scaria, P. V, Plank, C., and Szoka, F. C. (1997) Design, synthesis, and characterization of a cationic peptide that binds to nucleic acids and permeabilizes bilayers. *Biochemistry 36*, 3008–3017.

(46) Fernández-Carneado, J., Kogan, M. J., Van Mau, N., Pujals, S., López-Iglesias, C., Heitz, F., and Giralt, E. (2005) Fatty acyl moieties: improving Pro-rich peptide uptake inside HeLa cells. *J. Pept. Res. 65*, 580–590.

(47) Lanford, R. E., Kanda, P., and Kennedy, R. C. (1985) Induction of Nuclear Transport with a Synthetic Peptide Homologous to the SV40 T Antigen Transport Signal *46*.

(48) Chugh, A., and Cois, F. (2008) Cellular uptake of cell-penetrating peptides pVEC and transportan in plants ‡. *J. Pept. Sci.* 477–481.

(49) Rothbard, J. B., Kreider, E., VanDeusen, C. L., Wright, L., Wylie, B. L., and Wender, P. a. (2002) Arginine-rich molecular transporters for drug delivery: Role of backbone spacing in cellular uptake. *J. Med. Chem. 45*, 3612–3618.

(50) Pooga, M., Hällbrink, M., Zorko, M., and Langel, Ü. (1998) Cell penetration by transportan. *FASEB J. 12*, 67–77.

(51) Lindgren, M., Hällbrink, M., Prochiantz, A., and Langel, Ü. (2000) Cell-penetrating peptides. *TiPS 21*, 99–103.

(52) Lundberg, P., and Langel, Ü. (2003) A brief introduction to cell-penetrating peptides. *J. Mol. Recognit. 16*, 227–233.

(53) Langel, Ü. (Ed.). (2002) Cell-Penetrating peptides: Processes and Applications 1st ed., p 406. CRC Press, Boca Raton.

(54) Jones, S. W., Christison, R., Bundell, K., Voyce, C. J., Brockbank, S. M. V, Newham, P., and Lindsay, M. a. (2005) Characterisation of cell-penetrating peptide-mediated peptide delivery. *Br. J. Pharmacol. 145*, 1093–102.

(55) Hansen, M., Kilk, K., and Langel, Ü. (2008) Predicting cell-penetrating peptides. *Adv. Drug Deliv. Rev. 60*, 572–9.

(56) Bratkovič, T. (2009) Progress in phage display: evolution of the technique and its applications. *Cell. Mol. Life Sci. 67*, 749–767.

(57) Fuchs, S. M., and Raines, R. T. (2004) Pathway for Polyarginine Entry into Mammalian Cells. *Biochemistry 43*, 2438–2444.

(58) Vives, E., Richard, J., Rispal, C., and Lebleu, B. (2003) TAT Peptide Internalization: Seeking the Mechanism of Entry. *Curr. Protein Pept. Sci. 4*, 125–132.

(59) Hoyer, J., Schatzschneider, U., Schulz-Siegmund, M., and Neundorf, I. (2012) Dimerization of a cell-penetrating peptide leads to enhanced cellular uptake and drug delivery. *Beilstein J. Org. Chem. 8*, 1788–97.

(60) Richard, J. P., Melikov, K., Brooks, H., Prevot, P., Lebleu, B., and Chernomordik, L. V. (2005) Cellular uptake of unconjugated TAT peptide involves clathrin-dependent endocytosis and heparan sulfate receptors. *J. Biol. Chem. 280*, 15300–15306.

(61) Richard, J. P., Melikov, K., Vives, E., Ramos, C., Verbeure, B., Gait, M. J., Chernomordik, L. V, and Lebleu, B. (2003) Cell-penetrating peptides. A reevaluation of the mechanism of cellular uptake. *J. Biol. Chem. 278*, 585–90.

(62) Futaki, S., Suzuki, T., Ohashi, W., Yagami, T., Tanaka, S., Ueda, K., and Sugiura, Y. (2001) Arginine-rich peptides. An abundant source of membrane-permeable peptides having potential as carriers for intracellular protein delivery. *J. Biol. Chem. 276*, 5836–40.

(63) Suzuki, T., Futaki, S., Niwa, M., Tanaka, S., Ueda, K., and Sugiura, Y. (2002) Possible existence of common internalization mechanisms among arginine-rich peptides. *J. Biol. Chem. 277*, 2437–43.

(64) Torchilin, V. (2008) Intracellular delivery of protein and peptide therapeutics. *Drug Discov. Today Technol. 5*, 95–103.

(65) Deshayes, S., Morris, M. C., Divita, G., and Heitz, F. (2005) Cell-penetrating peptides: tools for intracellular delivery of therapeutics. *Cell. Mol. life Sci. 62*, 1839–1849.

(66) Wadia, J. S., Stan, R. V, and Dowdy, S. F. (2004) Transducible TAT-HA fusogenic peptide enhances escape of TAT-fusion proteins after lipid raft macropinocytosis. *Nat. Med. 10*, 310–315.

(67) Rothbard, J. B., Jessop, T. C., and Wender, P. a. (2005) Adaptive translocation: the role of hydrogen bonding and membrane potential in the uptake of guanidinium-rich transporters into cells. *Adv. Drug Deliv. Rev. 57*, 495–504.

(68) Stewart, K. M., Horton, K. L., and Kelley, S. O. (2008) Cell-penetrating peptides as delivery vehicles for biology and medicine. *Org. Biomol. Chem. 6*, 2242–55.

(69) Hughes, B. (2010) Antibody-drug conjugates for cancer: poised to deliver? *Nat. Rev. Drug Discov. 9*, 665–7.

(70) Robertson, K. L., Soto, C. M., Archer, M. J., Odoemene, O., and Liu, J. L. (2011) Engineered T4 viral nanoparticles for cellular imaging and flow cytometry. *Bioconjug. Chem. 22*, 595–604.

(71) Souza, G. R., Christianson, D. R., Staquicini, F. I., Ozawa, M. G., Snyder, E. Y., Sidman, R. L., Miller, J. H., Arap, W., and Pasqualini, R. (2006) Networks of gold nanoparticles and bacteriophage as biological sensors and cell-targeting agents. *Proc. Natl. Acad. Sci. U. S. A. 103*, 1215–20.

(72) Chonn, a, and Cullis, P. R. (1995) Recent advances in liposomal drug-delivery systems. *Curr. Opin. Biotechnol. 6*, 698–708.

(73) Kay, M. A., Glorioso, J. C., and Naldini, L. (2001) Viral vectors for gene therapy : the art of turning infectious. *Nat. Med. 7*, 33–40.

(74) Wu, A. M., and Senter, P. D. (2005) Arming antibodies: prospects and challenges for immunoconjugates. *Nat. Biotechnol. 23*, 1137–46.

(75) Mäe, M., Rautsi, O., Enbäck, J., Hällbrink, M., Aizman, K. R., Lindgren, M., Laakkonen, P., and Langel, Ü. (2012) Tumour Targeting with Rationally Modified Cell-Penetrating Peptides. *Int. J. Pept. Res. Ther. 18*, 361–371.

Chapter Two

Controlled Cellular Adhesion and Growth on Cell-imprinted Polyacrylamide Hydrogels

2.1 Introduction

Controlling mammalian cell adhesion and growth is critical to microscale tissue engineering and numerous biomedical research applications such as biosensor fabrication, applied cell biology, and high-throughput screening.[1–4] As previously discussed in Chapter 1, this can be accomplished through chemical-based cues or generating a well-defined surface topography. Chemical-based approaches to controlling mammalian cell adhesion often involve coating a non-adhesive surface with a small molecule,[5,6] carbohydrate,[7,8] membrane,[9] peptide,[10] nucleic acid,[11,12] protein,[13] or antibody[14] that binds natural or unnatural cell-surface receptors and adheres the cell to that surface. While these reagents effectively adheres cells to a substrate, they are often susceptible to environmental and enzymatic degradation, decreasing the shelf life of the substrate. Moreover, biopolymer and small molecule affinity reagents require separate synthesis, purification, and conjugation steps, which increase the overall complexity and cost of substrate fabrication.

Surface topography can have significant effects on cell adhesion and growth, influencing cell orientation, migration and organized cytoskeletal arrangements

through contact cue guidance.[15] Researchers have shown that well-defined surface features on engineered materials can influence cell adhesion and spreading over surface.[16] However, generating well-defined surface features often requires multi-step microfabrication protocols and specialized techniques.

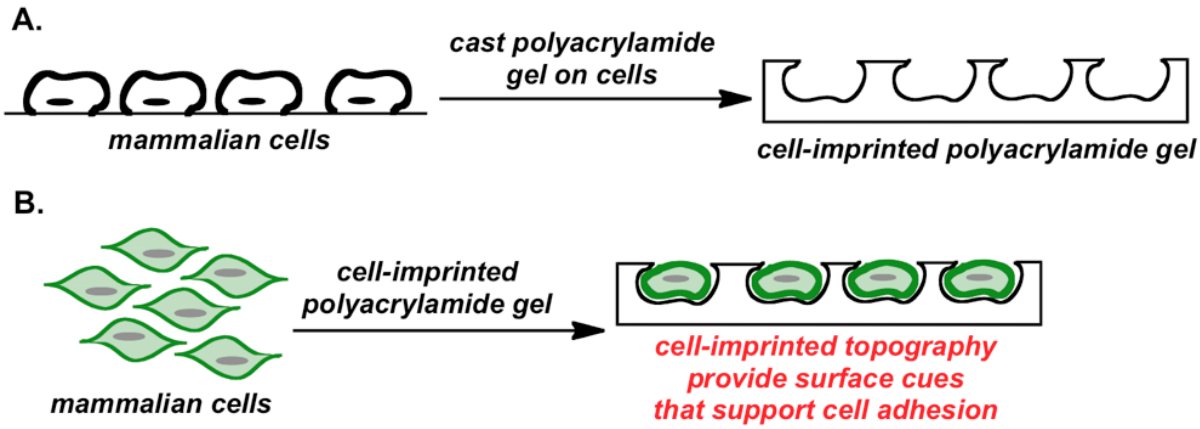

Figure 2.1. (A) Mammalian cells are cultured and fixed to tissue culture plates. Pre-mixed polyacrylamide solution is cast over the monolayer of cells, resulting in a cell-imprinted hydrogel. (B) Mammalian cells constitutively expressing green fluorescent protein (GFP) are cultured on the hydrogels and adhere due to surface topography cues.

We set out to identify a technique to prepare substrates for programmed cell adhesion and growth that doesn't rely on specialized or expensive equipment and does not require affinity reagents. Researchers have shown that bacterial or virus cell-imprinted features support the recognition of those cells from solution, and cell-imprinted detection platforms can be used within bioanalytical devices.[3] Inspired by this work, we examined the utility of mammalian cell-imprinted materials for programming cell growth on a hydrogel surface. A hydrogel would be cast onto a monolayer of adherent mammalian cells and would rely on cell-imprinted hydrogel surface features to guide cell adhesion and growth (Fig. 2.1). Hydrogels are inexpensive

and easy to prepare, are not cytotoxic, are permeable to oxygen and other soluble factors, have tunable mechanical properties, and can be made into virtually any conceivable shape, making them ideal substrates for cellular growth.

2.2 Developing cell-imprinted polyacrylamide gels

Cell-imprinted polyacrylamide hydrogels were poured over a monolayer of HeLa (human cervical cancer) cells grown in a 6-well tissue culture plate. Cells were incubated in a premixed solution consisting of 30% acrylamide, 1% bisacrylamide (wt/vol), tetramethylethylene-diamine (TEMED), and ammonium persulfate (APS) at room temperature. After a 20 minute incubation period, gels solidified. In an attempt to remove cellular debris, gels were incubated in a 1 M aqueous solution of sodium hydroxide for 1 hour at 37 °C followed by a 1 hour incubation in 0.6 M sodium dodecyl sulfate (SDS) at 37 °C. They were then rinsed three times with phosphate buffered saline (PBS) and topology of the gels characterized by scanning electron microscopy (SEM). As seen in Fig. 2.2A, our initial efforts resulted in the formation of cell-imprinted features on the surface of the hydrogel. However, the cell-imprinted features varied in dimension and a large amount of intact cells and remained attached to the cell-imprinted hydrogel surfaces. Intact cells and/or cell debris on the hydrogel surface, or within hydrogel matrix, were stained by Coomassie, which indiscriminately stains

amino acid polymers (Fig. 2.2B).

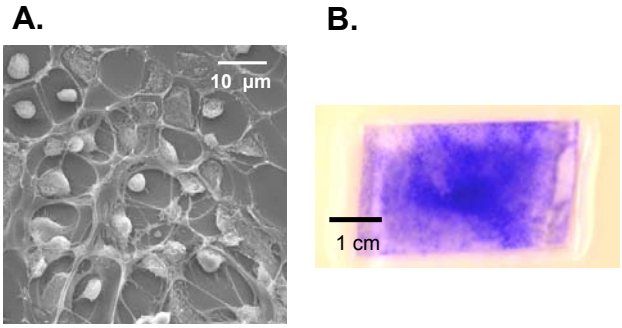

Figure 2.2. (A) Scanning electron microscope (SEM) images indicated that initial attempts resulted in non-uniform and irregular formation of imprints as well as the remnants of whole cells and cellular debris. (B) A HeLa cell imprinted hydrogel stained with Coomasie indicates the presence of a significant amount of cells and cellular debris.

We hypothesized that fixing the cells before the casting the gels would help to maintain uniform cell morphology throughout the solidification process and prevent changes in cell shape or cell detachment. As a result, cell imprints should be more regular in size and shape, and therefore more accurately represent physical features of the imprinted cell. In addition, pre-fixing cells should result in less cell debris becoming trapped within the gel matrix or on the imprinted surface. In order to test this, we proceeded with the imprinting process using cells with epithelial-like and fibroblast-like morphology. Cell-imprinted polyacrylamide gels were prepared from subconfluent monolayers of HeLa (human cervical cancer, epithelial-like morphology), HEK-293T (human embryonic kidney, epithelial-like morphology), and MRC-9 (human embryonic lung, fibroblast- like morphology) cells grown in a 6-well tissue culture plate. Cells were first fixed with a 4% formaldehyde/PBS solution for five minutes, then incubated in a pre-mixed solution containing 30% acrylamide, 1% bisacrylamide (wt/vol), TEMED,

and APS at 37 °C. Cell-imprinted gels were then incubated in a 0.25% trypsin solution for 1 hour at 37 °C, washed three times with PBS, incubated in a 1 M aqueous hydrochloric acid solution for 6 hours at 37 °C, and washed an additional three times with PBS. Gels were then stored in PBS at 4 °C.

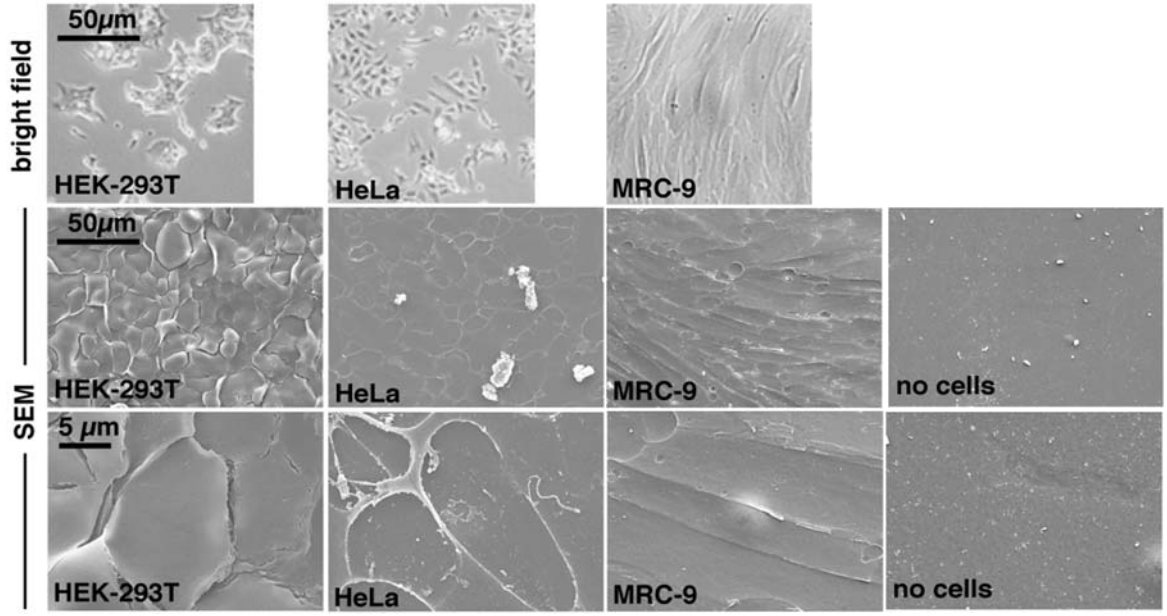

Figure 2.3. *Top*-Bright-field images of HEK-293T, HeLa, or MRC-9 cells grown on polystyrene tissue culture plates. *Middle and Bottom*- Scanning Electron Microscope (SEM) images of polyacrylamide hydrogels imprinted with fixed HEK-293T, HeLa, or MRC-9 cells washed with 0.25% trypsin for 1 hour, 1M hydrochloric acid for 6 hours. *Right*- SEM images of non-imprinted polyacrylamide hydrogels

Following cell-imprinting and washing, gels were characterized by SEM. Consistent with our hypothesis, features on the surface of cell-imprinted polyacrylamide hydrogels correlated well with the size and morphology of the imprinting cell (Fig. 2.3). For example, HeLa cells and HEK-293T cells have epithelial-like morphology, are polygonal in shape with regular dimensions and typically grow in discrete patches. Imprints generated from HeLa and HEK-293T cells matched these features: they contain both elliptical and polygonal features. In contrast, MRC-9 cells have fibroblast-like

morphology, are bipolar with an elongated shape and typically do not grow in discrete clusters. Cell-imprinted featured generated from MRC-9 cells are elongated and fibrous, and generally match the morphology of MRC-9 cells. In contrast, polyacrylamide hydrogels cast onto a cell culture plate lacking cells do not have well-defined surface features. SEM images of gels washed sequentially with trypsin and hydrochloric acid solutions do not have appreciable levels of intact cells and/or cell debris on their surface.

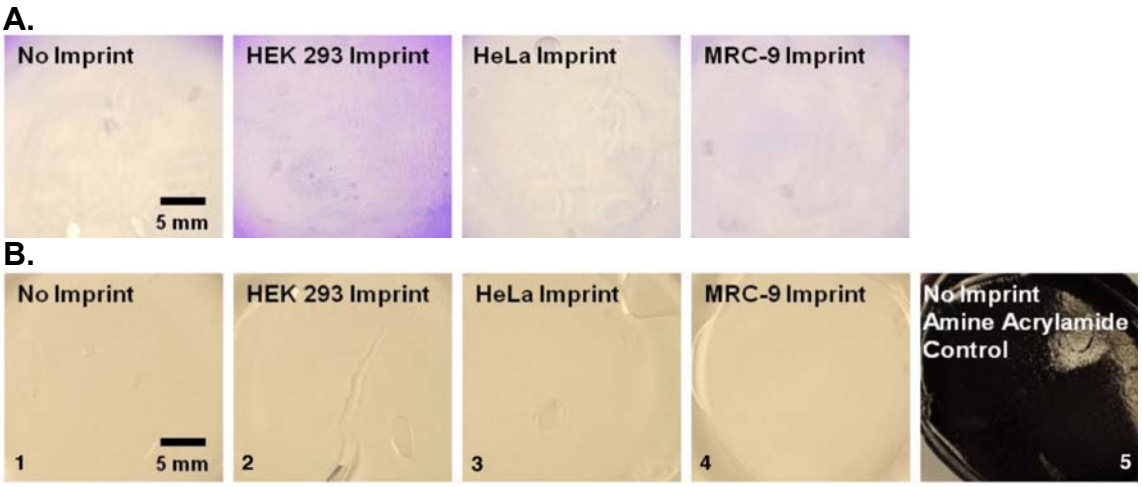

Figure 2.4. (A) Cell-imprinted polyacrylamide hydrogels washed with 0.25% trypsin for 1 hour at 37 °C then 1M hydrochloric acid for 6 hours at 37 °C. Hydrogels were then stained with Coomasie and destained. Imprinted areas of the gels do not show appreciable staining by Coomasie. (B) Imprinted hydrogels treated in the same manner as those in (A) do not show appreciable staining by ninhydrin (gels 1-4) compared to amino-functionalized hydrogels prepared with poly-N-3-(aminopropyl)-methyacrylamide (gel 5).

In addition, these gels did not stain with Coomassie. Collectively, these data indicate that cells and/or cell debris is not present in the gel matrix or on the gel surface (Fig. 2.4A). Amines present in cell surface proteins containing lysine or aminoglycans would be expected to stain with ninhydrin. While non-imprinted amino-functionalized hydrogels

prepared with poly-N-3-(aminopropyl)-methacrylamide did stain with ninhydrin, cell-imprinted polyacrylamide gels did not (Fig. 2.4B). These data suggest that significant levels of cell surface and/or peptide/protein debris are not present in the gel matrix or on the gel surface. Therefore, cell adhesion and growth on cell-imprinted polyacrylamide hydrogels is likely the result of surface contact cue guidance and not due to interactions involving cell debris on the gel surface.

2.3 Adhesion of mammalian cells to cell-imprinted surfaces

In order to determine if cell-imprinted features support the adhesion of mammalian cells, we treated HeLa, HEK-293T and MRC-9-imprinted polyacrylamide gels with either HeLa–GFP, HEK-293T–GFP, or MRC-9 cells. HeLa–GFP and HEK-293T–GFP constitutively express green fluorescent protein (GFP). Therefore, fluorescence on the gel surface indicates the adhesion of these cells. Attachment of MRC-9 cells, which do not constitutively express GFP, was detected by staining the hydrogel with DAPI, which identifies the nuclei of cells. Cell-imprinted gels were prepared as described above, then washed once with the corresponding cell media. Cell-imprinted gels and non-imprinted gels were then seeded with either HeLa–GFP, HEK-293T–GFP, (both in Dulbecco's modified Eagle medium (DMEM) containing 10% Fetal Bovine Serum (FBS)) or MRC-9 cells (in a RPMI/10% FBS solution) and incubated at 37 °C in a 5% carbon dioxide environment for 12 hours. After incubation, the gels

were washed three times with their respective media to remove any non-adherent cells. Fluorescence images of gels treated with HeLa–GFP or HEK-293T were obtained on a Typhoon Trio imager.

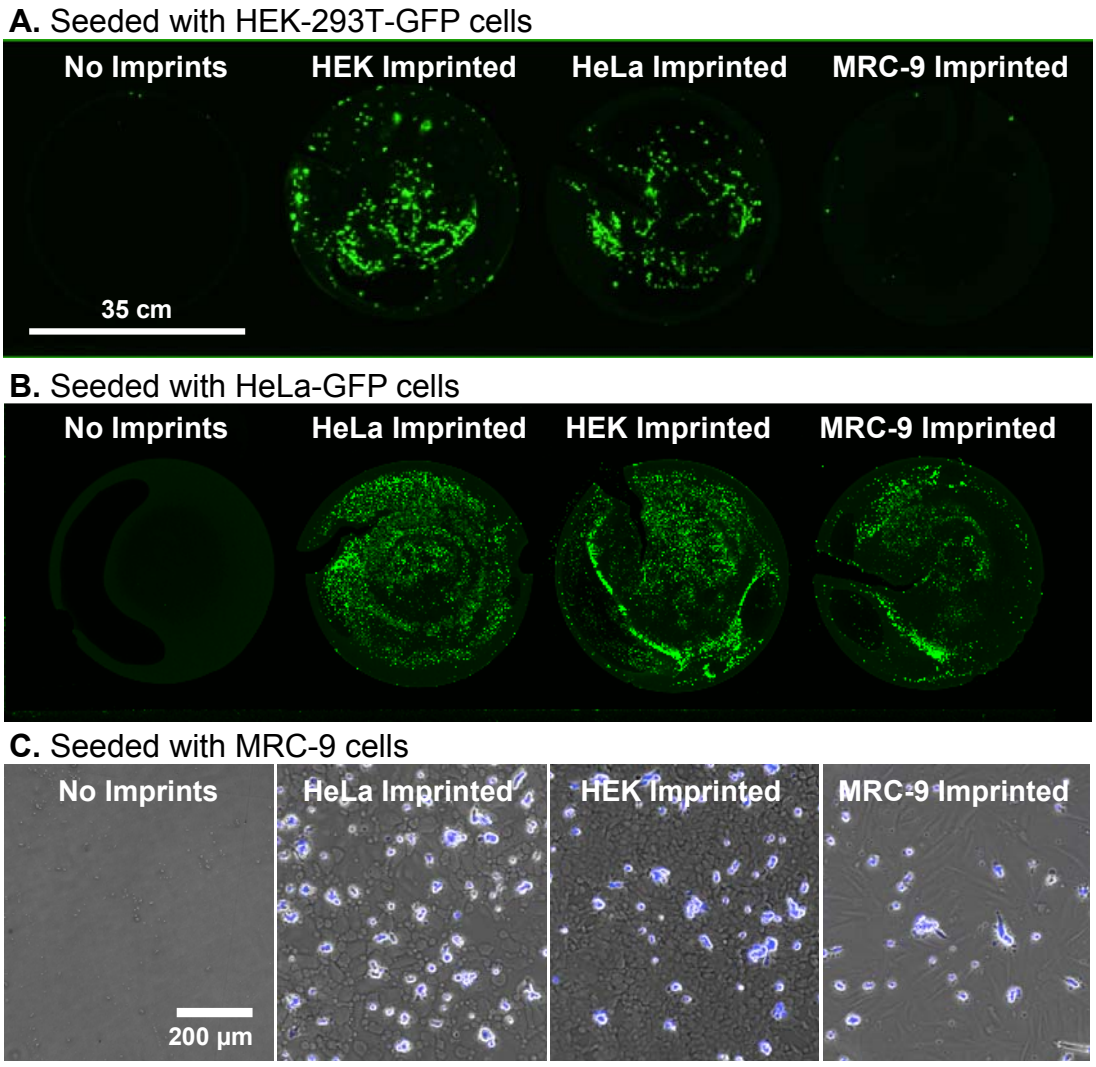

Figure 2.5. Washed cell-imprinted polyacrylamide hydrogels were seeded with (A) HEK-293T-GFP, (B) HeLa-GFP, or (C) MRC-9 cells and imaged to determine if cell adhesion occurred. Images for (A) and (B) were taken using a Typhoon Trio imager. (C) Cells were stained with DAPI and imaged through fluorescence microscopy.

As shown in Fig. 2.5, polyacrylamide gels lacking cell-imprinted surface features do not support the adhesion of any cell line tested. However, HeLa, HEK-293T, and MRC-9

cell-imprinted polyacrylamide gels are a substrate for HeLa–GFP cell adhesion. HeLa cells are cervical cancer cells, and adhere to and grow on a wide array of surfaces.[17] Therefore, it is unsurprising that HeLa cells adhere to all three cell-imprinted surfaces. HEK-293T–GFP cells adhere to HEK- 293T cell-imprinted and HeLa cell-imprinted polyacrylamide gels, which contain epithelial-like imprinted features with elliptical and polyhedral imprints with regular dimensions. However, HEK-293T–GFP cells did not adhere to MRC-9 cell-imprinted polyacrylamide gels, which contain fibroblast-like imprinted features with elongated and fibrous structure. MRC-9 cells adhered to HeLa, HEK-293, and MRC-9-imprinted hydrogels.

Interestingly, MRC-9 cells grew on all cell-imprinted surfaces, but appeared to adhere best to HeLa and HEK-293T-imprinted hydrogels. In addition, unlike MRC-9 cells grown cell culture plates, cells grown on cell-imprinted hydrogels do not appear to have fibroblast-like morphology. Collectively, these data support our hypothesis that cell-imprinted features support the adhesion of various mammalian cells. In at least one case, change in cell-imprinted topography dramatically affects cell adhesion. Therefore, in some cases cell-imprinted topography may be useful for programming cell-selective adhesion to a surface. None of the cell lines tested adhered to any cell-imprinted gel in the absence of fetal bovine serum. This suggests that serum protein is required for cell adhesion and growth within cell-imprinted features.

In order to test the viability of cells adhered to cell-imprinted hydrogels, we treated HeLa, HEK-293T and MRC-9 cells grown on their respective imprinted gels with MTT cell viability reagent 72 hours after cell seeding. In each case, all adherent cells stained following MTT treatment (Fig. 2.6). These data, combined with DAPI staining of MRC-9 cells in Fig. 2.1C indicate that all cells tested are viable when grown on cell-imprinted hydrogels.

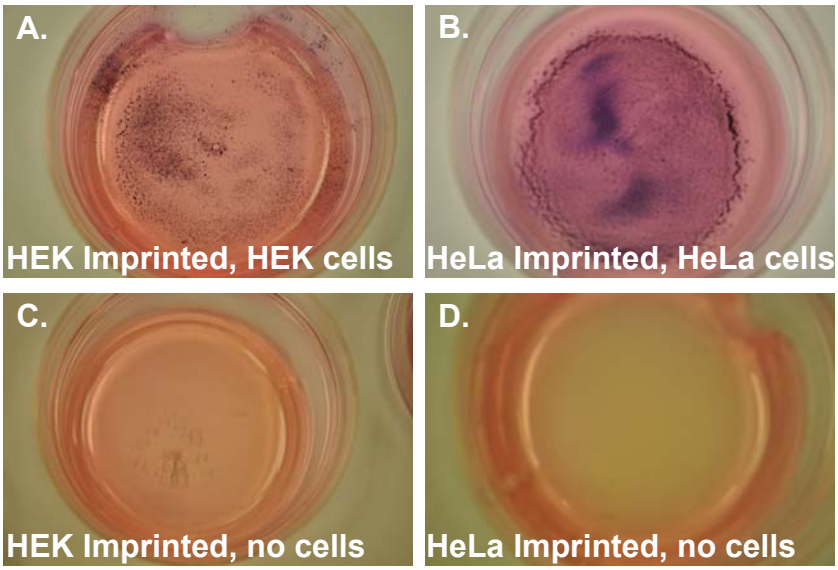

Figure 2.6. Cell-imprinted polyacrylamide hydrogels seeded with (A) HEK-293T, (B) HeLa, or (C & D) no cells treated with TACS® MTT reagent stains cells grown in cell-imprinted features, but does not stain non-seeded hydrogels.

2.4 Controlling patterned growth on hydrogel surfaces

We hypothesized that spatially defined cell imprints on a tissue culture plate could be used to pattern cell-imprinted features, which could potentially program the

assembly and adhesion of cells from solution onto a hydrogel surface. In order to avoid methods that rely on specialized and/or expensive equipment, we focused on the development of an inexpensive and experimentally simple way to fabricate patterned cell-imprinted surfaces on a tissue culture plate and hydrogel surface. We prepared a checkerboard pattern on a polystyrene tissue culture plate using 0.5 cm^2 squares of UGlu™ tape - a multi-purpose adhesive that is easily applied to and removed from polystyrene surfaces. HeLa cells were then added to the checkerboard-patterned surface; we observed that cells did not grow on taped regions but did grow on regions of the polystyrene tissue culture plate around it. The adhesive was removed and a polyacrylamide gel was cast on the checkerboard-patterned cells, thereby generating a polyacrylamide gel with a well-defined checkerboard pattern of HeLa cell-imprinted features (summarized in Fig. 2.7A). After washing the cell-imprinted hydrogel as described above, HeLa–GFP cells were seeded onto the gel and incubated in DMEM/10% FBS for 12 hours at 37 °C/5% CO_2. The gel was then washed with DMEM to remove unbound cells, and bound cells were allowed to grow for an additional 12 or 36 hours. The entire gel was washed briefly with PBS and cell fluorescence on the surface of each gel was imaged.

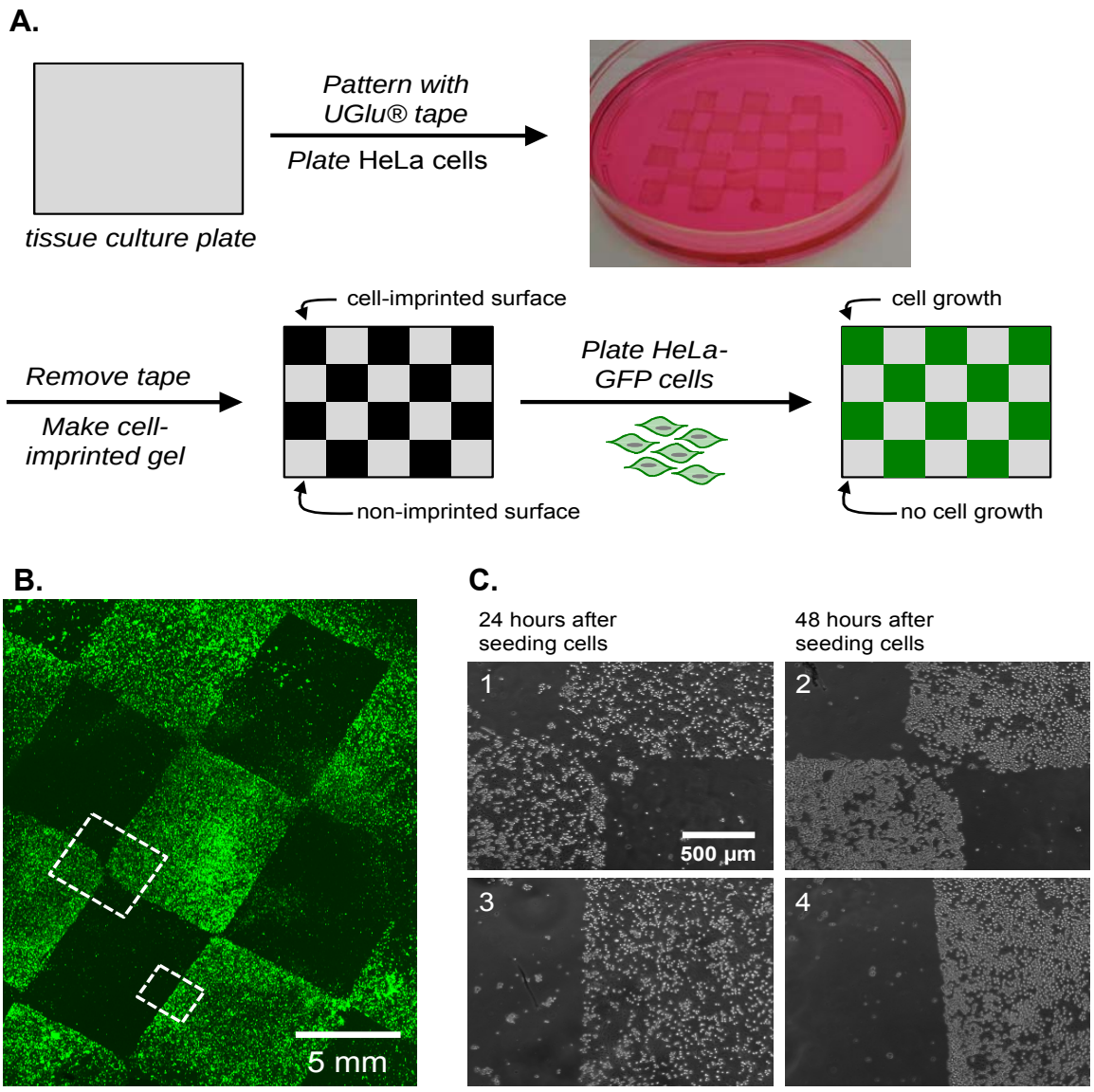

Figure 2.7. (A) Using UGlu® tape, HeLa cells were grown in a checkerboard pattern on a polystyrene tissue culture dish. At 80% confluency, tape was removed and a polyacrylamide hydrogel cast, creating spatially-defined cell imprints. Hydrogels were then seeded with HeLa-GFP cells. (B) Fluorescence image of a patterned cell-imprinted hydrogel seeded with HeLa-GFP cells. Dotted boxes represent images shown in (C) of growth at 24 or 48 hours.

Consistent with our previous findings, high densities of HeLa–GFP cells were observed in areas containing cell-imprinted features. In contrast, appreciable levels of HeLa–GFP cells were not observed in areas lacking cell-imprinted features (Fig. 2.7B). Importantly, cell density increased over time within cell-imprinted regions, but did not expand into

non-imprinted regions (Fig. 2.7C). Cell counting indicates that cell densities on hydrogels are similar to those observed on polystyrene cell culture plates.

2.5 Conclusion

Using a relatively simple and inexpensive procedure, we have shown that cell-imprinted features can serve as contact cues that support cell adhesion and growth. In one case, the topology of cell-imprinted features dramatically affected cell adhesion and growth. Collectively, these data show that cell-sized topological features can support cell adhesion and potentially could be used to control cell-selective adhesion and growth. We have demonstrated the ability to program cell patterning on a hydrogel surface simply through cell-imprinting. We observed dense cell growth within cell-imprinted regions, and cell growth remained tightly confined to those regions. Cell-imprinting may represent a simple and inexpensive alternative to generating hydrogel or elastomer surfaces that support cell adhesion and growth. Since cell-imprinted polyacrylamide hydrogels are fabricated without the use of lithography or other specialized equipment and/or techniques, do not require biopolymer affinity reagents, and are prepared from inexpensive materials, this method may find more general use in fields including tissue engineering, diagnostics and biomaterials science.

2.6 Materials and Methods

Mammalian cell culture

HEK293T, HEK 293T–GFP, HeLa and HeLa–GFP cells were cultured in high glucose Dulbecco's modified Eagle medium (DMEM) with 10% Fetal Bovine Serum (FBS) in a 37 °C incubator, 5% CO2 environment. Human embryonic lung fibroblasts (MRC-9) were cultured in RPMI-1640 media and 10% FBS in a 37 °C incubator, 5% CO2 environment.

Cell-imprinted hydrogel fabrication

Cells were grown in a 6-well tissue culture dish until approximately 80% confluency. They were washed once with 37 °C phosphate buffered saline (PBS), fixed with 4% paraformaldehyde in 37 °C PBS for 5 minutes, and washed twice with 37 °C PBS. Polyacrylamide gels were prepared by mixing 5.33 mL of a 31% acrylamide solution (30% acrylamide and 1% bisacrylamide (wt/vol)) with 2.0 mL PBS and 0.5 mL RNase/DNase free-water. Gelation was initiated by the addition of 8 μL of TEMED and 80 μL of APS, followed by gentle mixing. 1.5 mL of the polyacrylamide solution was added to fixed cells in a 6-well tissue culture dish and incubated at 37 °C/5% CO2 for 20 minutes. The hydrogels were then removed from the cell culture dish, placed cell-imprint up in another 6-well plate and each gel was incubated with 3 mL of 0.25% trypsin solution for 1 hour at 37 °C. Following trypsin treatment, gels were washed three times with room temperature PBS and then treated with 1 M aqueous HCl for 6

hours at 37 °C. Hydrogels were then washed three times with room temperature PBS, and incubated overnight in PBS at 37 °C/5% CO2.

Mammalian cell growth on cell-imprinted hydrogels

Cell-imprinted hydrogels were washed twice with 37 °C high glucose Dulbecco's modified Eagle medium (DMEM). 2 mL of DMEM/10% FBS containing either HEK 293T–GFP or HeLa–GFP cells was added to each gel containing approximately 3.0×10^5 cells per mL. The gels were incubated overnight at 37 °C and 5% CO2. Hydrogels were then washed twice with 5 mL of 37 °C DMEM to remove any dead or non-adhered cells. Cells typically grew on the cell-imprinted hydrogels for 1–4 days before imaging.

REFERENCES

(1) Bures, P., Huang, Y., Oral, E., and Peppas, N. a. (2001) Surface modifications and molecular imprinting of polymers in medical and pharmaceutical applications. *J. Control. Release 72*, 25–33.

(2) Hench, L. L., and Polak, J. M. (2002) Third-generation biomedical materials. *Science 295*, 1014–7.

(3) Hillberg, a L., Brain, K. R., and Allender, C. J. (2005) Molecular imprinted polymer sensors: implications for therapeutics. *Adv. Drug Deliv. Rev. 57*, 1875–89.

(4) Khademhosseini, A., Langer, R., Borenstein, J., and Vacanti, J. P. (2006) Microscale technologies for tissue engineering and biology. *Proc. Natl. Acad. Sci. U. S. A. 103*, 2480–7.

(5) Rothbard, J. B., Jessop, T. C., and Wender, P. a. (2005) Adaptive translocation: the role of hydrogen bonding and membrane potential in the uptake of guanidinium-rich transporters into cells. *Adv. Drug Deliv. Rev. 57*, 495–504.

(6) Lee, J. H., Pazk, J. O. I. W., and Lee, H. B. (1991) Cell adhesion and growth on polymer surfaces with hydroxyl groups prepared by water vapour plasma treatment *12*, 443–448.

(7) Lopina, S. T., Wu, G., Merrill, E. W., and Griffith-Cima, L. (1996) Hepatocyte culture on carbohydrate-modified star polyethylene oxide hydrogels. *Biomaterials 17*, 559–69.

(8) Griffith, L. G., and Lopina, S. (1998) Microdistribution of substratum-bound ligands affects cell function: hepatocyte spreading on PEO-tethered galactose. *Biomaterials 19*, 979–86.

(9) Groves, J. T., Mahal, L. K., and Bertozzi, C. R. (2001) Control of Cell Adhesion and Growth with Micropatterned Supported Lipid Membranes 5129–5133.

(10) Orner, B. P., Derda, R., Lewis, R. L., Thomson, J. a, and Kiessling, L. L. (2004) Arrays for the combinatorial exploration of cell adhesion. *J. Am. Chem. Soc. 126*, 10808–9.

(11) Hsiao, S. C., Shum, B. J., Onoe, H., Douglas, E. S., Gartner, Z. J., Mathies, R. a, Bertozzi, C. R., and Francis, M. B. (2009) Direct cell surface modification with DNA for the capture of primary cells and the investigation of myotube formation on defined patterns. *Langmuir 25*, 6985–91.

(12) Selden, N. S., Todhunter, M. E., Jee, N. Y., Liu, J. S., Broaders, K. E., and Gartner, Z. J. (2012) Chemically programmed cell adhesion with membrane-anchored oligonucleotides. *J. Am. Chem. Soc. 134*, 765–8.

(13) Keselowsky, B. G., Collard, D. M., and García, A. J. (2003) Surface chemistry modulates fibronectin conformation and directs integrin binding and specificity to control cell adhesion. *J. Biomed. Mater. Res. A 66*, 247–59.

(14) Pierres, A., Tissot, O., Malissen, B., and Bongrand, P. (1994) Dynamic adhesion of CD8-positive cells to antibody-coated surfaces: the initial step is independent of microfilaments and intracellular domains of cell-binding molecules. *J. Cell Biol. 125*, 945–53.

(15) Jiang, X., Takayama, S., Qian, X., Ostuni, E., Wu, H., Bowden, N., LeDuc, P., Ingber, D. E., and Whitesides, G. M. (2002) Controlling Mammalian Cell Spreading and Cytoskeletal Arrangement with Conveniently Fabricated Continuous Wavy Features on Poly(dimethylsiloxane). *Langmuir 18*, 3273–3280.

(16) Kim, E. K. F., Reano, R. M., Pang, S. W., Yee, A. F., Chen, C. S., and Leong, K. W. (2005) Nanopatterned-induced changes in morphology and motility of smooth muscle cells. *Biomaterials 26*, 5405–5413.

CHAPTER THREE

MULTIVALENCY EFFECTS ON THE POTENCY AND CELL-SELECTIVITY OF CELL-PENETRATING PEPTIDES

3.1 Introduction

Various technologies have been developed to deliver exogenous cargo to cells in therapeutic and imaging settings. However, there is often a trade-off between the ability to selectively bring cargo to a cell and the ability to promote internalization of said cargo. This chapter describes our attempts to develop a delivery vehicle capable of selectively transporting to and internalizing exogenous cargo in PC-3 prostate cancer cells.

3.2 Developing a Cell-Selective Cell-Penetrating Peptide to Target PC-3 Prostate Cancer Cells

Prostate cancer is the second most common form of cancer in American males. Current diagnostic methods and treatments rely heavily on the presence of prostate-specific membrane antigen (PSMA) as increased expression levels of the protein have been shown to correlate with the presence of cancerous cells[1,2]. Targeted delivery to prostate cancer cells depends on the use of tools such as antibodies and/or fragment antigen-binding regions (Fab fragments) that recognize PSMA[3]. As previously discussed, however, these tools are limited in that they can only transport their cargo to

a close proximity of the target cells without being able to promote internalization any further than depending on the increase metabolism of the unhealthy cells. In addition to this, not all prostate cancer cell lines express/display PSMA or express them at elevated levels[2]. This further limits the ability of current tools to more effectively treat the disease. We therefore sought to develop a delivery vehicle that would not depend on the presence of PSMA and used PSMA-negative PC-3 metastatic prostate cancer cells as the target cell line.

Inherent limitations of cargo delivery facilitated by antibodies, such as ease and cost of production, shelf-life, and inability to cross the cellular membrane, have been overcome with the discovery and study of cell-penetrating peptides (CPPs) or protein transduction domains (PTDs)[4,5]. These CPPs are comparatively easier to produce than antibodies and Fab fragments and have been shown to enter cells when applied externally[6–8]. Like antibodies, they are non-cytoxic, but due to their smaller size (generally <30 amino acids long) have shown to have an increased circulation period *in vivo*[9]. Unlike antibodies, most cell-penetrating peptides are incapable of selectively targeting a single cell line. Many CPPs have a highly cationic structure that allow it to interact with negative charges on cell-surfaces, making many indiscriminant when entering a cell[10]. Using this knowledge, we aimed to develop a tool capable of delivering cargo to a cell with the specificity of antibodies and the internalization capabilities of cell-penetrating peptides through the use of phage display.

Phage display has primarily been used to study functional and structural properties of known protein domains[11]. Recently, its application has widely expanded. Perhaps its most well-known use is through the display of Fab fragments. Antibody libraries have been constructed by splicing in random heavy and light chains, each pair forming unique antibody fragments[12]. These can be amplified and screened against antigens for high affinity binding to a target molecule or receptor[13] and used to develop the field of targeted drug delivery[14,15]. This same principle was utilized while searching for a synthetic CPP capable of targeting and entering PC-3 cells without depending on interactions with a specific receptor or cell-surface protein.

A phage-display library was prepared and several rounds of screening were performed to isolate the CPP that displayed internalization specificity for PC-3 cells (Figure 3.1). First, a tissue culture plate displaying a monolayer of carboxylic acids was treated with the library to remove and phage with a high positive net charge. It is these CPPs that often enter cells indiscriminately as their charge increases their likelihood of binding the negatively charged cell surface and facilitating uptake. The remaining unbound candidates of the library were then incubated with a monolayer of PC-3 cells (positive selection). Cells were washed five times with PBS, then three times with Tris-buffered saline (TBS)/0.1 % Tween-20 solution. They were then treated with 3 mg/mL subtilisin in TBS for 40 minutes at 4 °C, removing any remaining cell-surface-bound phage through proteolytic degradation and making the phage non-infective. Following

subtilisin treatment, cells were washed and additional three times with PBS containing protease inhibitor cocktail and pelleted by centrifugation. Cells were lysed open and any internalized phage were amplified in *Escherichia coli*.

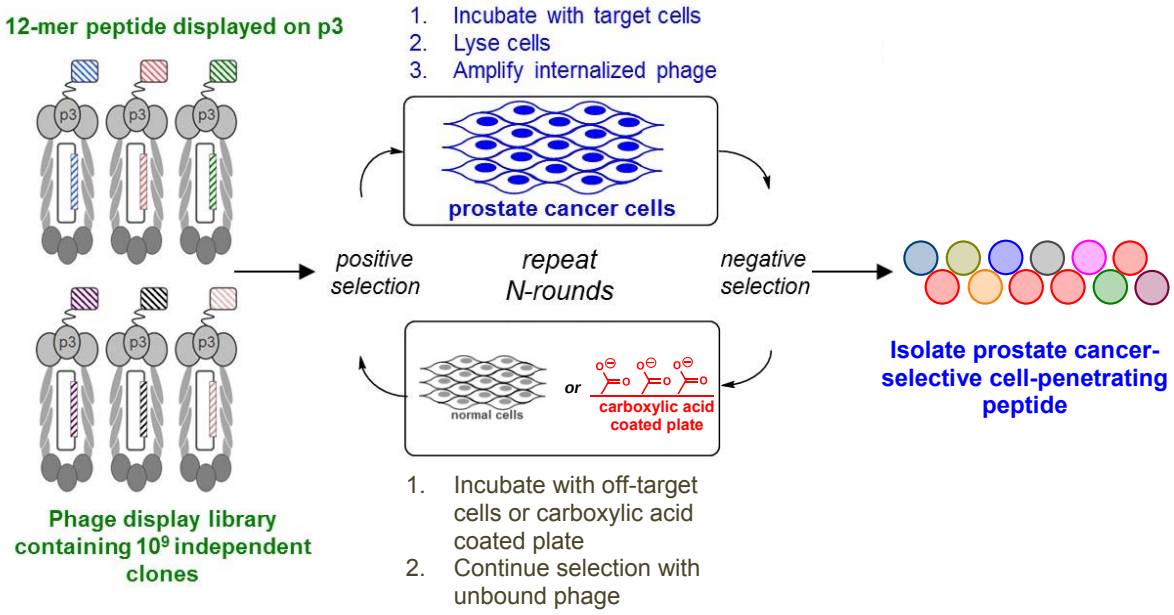

Figure 3.1 Phage panning for a PC-3 prostate cancer cell-selective protein transduction domain. Phage are incubated with PC-3 prostate cancer cells and enriched for cell-penetration. Cell-penetrating phage are then incubated with off-target cell lines, and phage that are not internalized by off-target cells or bound by negative charges are moved on to another round of selection.

These phage were then incubated with four different off-target, negative selection, cell lines and any unbound/non-internalized phage were collected. This process of negative and positive selection was repeated three more times to find the most selective and potent molecule. The remaining phage were then collected, amplified in *E. coli,* and grown as individual plaques on agar plates. Single plaques were picked and grown in Luria Broth (LB), ssDNA isolated, and sequenced. The sequence that presented itself

most often was termed "Ypep" (N-YTFGLKTSFNVQ-C) with no sequence homology to other sequences that survived the rigorous rounds of screening.

3.3 Evaluating Ypep-fusion Protein Uptake

In order to quantitatively analyze the specificity and efficacy of Ypep, super-folder green fluorescent protein (sfGFP) was utilized as a reporter protein as it can be easily imaged through fluorescence microscopy. A fusion protein of Ypep-$(GGS)_4$-sGFP was prepared (henceforth refered to as Ypep-GFP) and its ability to enter PC-3 cells was tested.

PC-3 cells were treated with 0.5, 1, 5, or 10 μM Ypep-GFP solution. Following a three hour incubation, the solution was removed, and cells were washed three times with a PBS solution containing 20 U/mL heparin sulfate, previously shown to be effective in removing surface-bound protein.[16–19] Cells were then trypsinized and assayed for internalized Ypep-GFP by flow cytometry. As shown in Figure 3.2 D, aconcentration-dependent increase in Ypep-GFP levels in PC-3 prostate cancer cells was observed. Through flow cytometry, ~42- and ~86-fold increase in fluorescence in cells following treatment with 5 or 10 μM Ypep-GFP, respectively, was found when compared to cells treated with similar concentrations of GFP alone. Fluorescence microscopy images show internalized Ypep-GFP in PC-3 cells following treatment with

10 μM Ypep-GFP (Figure 3.2B). In contrast, no appreciable fluorescence was observed in cells treated with 10 μM GFP, and imaged under the same conditions (Figure 3.2A). These data indicate that Ypep is indeed capable of facilitating protein uptake in prostate cancer cells.

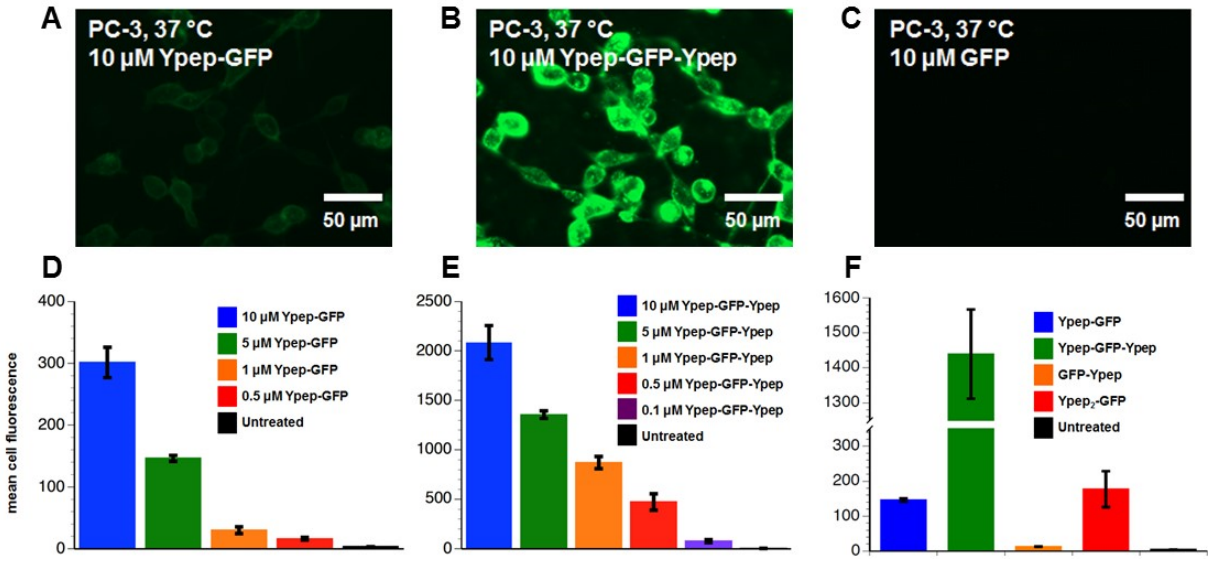

Figure 3.2 Comparing GFP uptake of Ypep fusion proteins in PC-3 cells. (A-C) Fluorescence microscopy images of PC-3 cells after a 1 hour treatment with 10 μM GFP, Ypep-GFP, or Ypep-GFP-Ypep. All images were taken using an EVOS fl fluorescence microscope at 20 % lamp intensity, 500 ms exposure. (D-E) Amounts of internalized GFP in PC-3 cells after treatment with 0.1, 0.5, 1, 5, or 10 μM Ypep-GFP or Ypep-GFP-Ypep as quantitated by flow cytometry. (F) Direct comparison of GFP uptake in PC-3 cells treated with 5 μM Ypep-GFP, Ypep-GFP-Ypep, GFP-Ypep or $Ypep_2$-GFP after a 3 hour incubation. Values and error bars represent the mean and standard deviation of three independent experiments.

3.4 Multivalency Effects Increase Cellular Uptake of Ypep-fusion Proteins

PC-3 prostate cancer cells treated with solutions of Ypep-GFP displayed only modest cellular uptake of the fusion protein (Figure 3.2D). Because our initial screen for a potent, cell-selective, cell-penetrating peptide utilized phage-display, where 5 copies

of Ypep are presented on the N terminus of the minor coat protein3 (p3), it was reasoned that perhaps multivalent display may be needed to facilitate highly potent Ypep-dependent delivery. Multivalency effects play critical roles in various biological processes[20] and has been been previously reported to contribute to the mechanism of uptake for a known CPP[21].

To determine what role multivalency plays in the uptake of Ypep protein fusions, a fusion protein with Ypep on the N and C termini of GFP (Ypep-GFP-Ypep) was prepared. PC-3 cells were then treated with solutions of 0.1-10 μM Ypep-GFP-Ypep, washed as previously described to remove cell-surface-bound proteins, trypsinized from the tissue culture plate, and GFP uptake measured by flow cytometry. As shown in Figure 3.2E, a concentration-dependent increase in Ypep-GFP-Ypep delivery in PC-3 cells was again observed. This increase in GFP delivery was further confirmed by comparing microscopy images of cells treated with 10 μM Ypep-GFP (Figure 3.2B) to cells treated with the same concentration of Ypep-GFP-Ypep (Figure 3.2C). GFP fluorescence increased by ~29-fold in PC-3 cells treated with 0.5 μM Ypep-GFP-Ypep when compared to PC-3 cells treated with the same concentration of Ypep-GFP. Moreover, PC-3 cells treated with 0.5 μM Ypep-GFP-Ypep exhibited ~3-fold higher GFP fluorescence than cells treated with 5 μM Ypep-GFP. Interestingly, when testing a GFP fusion with Ypep displayed only on the C-terminus, GFP-Ypep, no GFP

uptake was observed, further suggesting that multivalency plays a key role in the potency of Ypep-dependent delivery.

3.5 Comparing the Efficacy of Ypep with Commercially Available CPPs

There are several commercially available CPPs and we set out to compare their ability to facilitate protein uptake in PC-3 cells with Ypep. GFP fusion proteins containing either a single N-terminal fusion with Tat or penetratin and $(GGS)_4$ linker (referred to as Tat-GFP and Pen-GFP, respectively)were prepared. In addition, we prepared GFP fusion proteins containing N- and C-terminal Tat or penetratin (referred to as Tat-GFP-Tat and Pen-GFP-Pen, respectively). We began by testing GFP uptake with monovalent display of the fusion proteins. PC-3 cells were treated with solutions containing 5 μM Ypep-GFP, Tat-GFP, or Pen-GFP. Cells were washed to remove cell-surface-bound proteins, as previously described, and GFP fluorescence was measured by flow cytometry. Treatment with this concentration of fusion protein resulted in the delivery of comparatively similar levels of Ypep-GFP and Pen-GFP to PC-3 cells. However, appreciable levels of Tat-GFP were not observed at the same concentration. Next we tested the bivalent constructs for GFP uptake. PC-3 cells were incubated with solutions of 100 nM Ypep-GFP-Ypep, Tat-GFP-Tat, or Pen-GFP-Pen. While bivalent display of Ypep resulted in a ~20-fold increase in GFP delivery over treatment with the

monovalent display, the same effect was not observed for Pen-GFP-Pen and Tat-GFP-Tat fusions (Figure 3.3B).

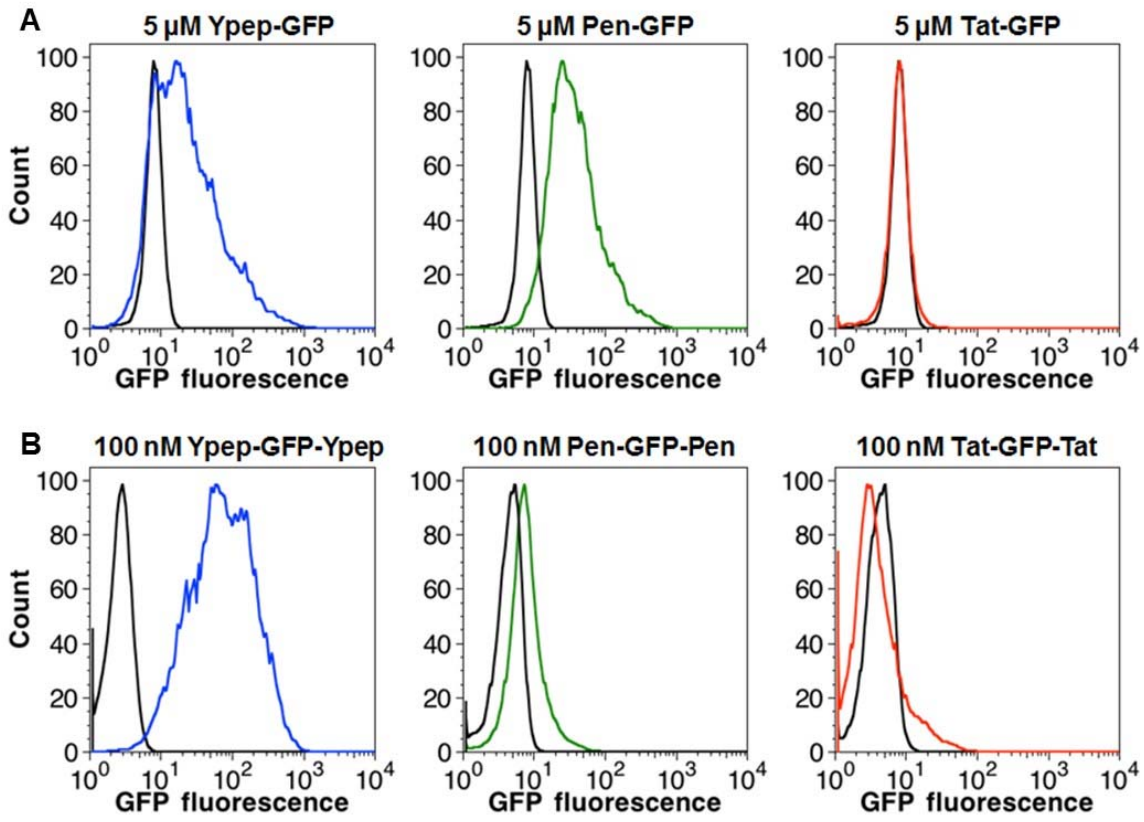

Figure 3.3 Comparing the uptake potency of Ypep, Tat, and penetratin. (A) Flow cytometry data showing amounts of internalized GFP in PC-3 cells after treatment with 5 μM Ypep-GFP (blue), penetratin-GFP (green), or Tat-GFP (red). (B) Flow cytometry data showing amounts of internalized GFP in PC-3 cells after treatment with 100 nM Ypep-GFP-Ypep (blue), penetratin-GFP-penetratin (green), or Tat-GFP-Tat (red). In each figure, untreated cells are represented in black, and colored lines represent treated cells.

It has been previously reported that 4-5 copies of Tat and as many as 10-50 copies of penetratin are required for a significant increase in the potency of uptake when compared to the potency of delivery observed for a monomeric fusion.[22] In contrast, we observe a dramatic increase in the potency of delivery for GFP fusions displaying only

two copies of Ypep. These data show the unique role multivalency plays on the potency of Ypep-dependent delivery of GFP.

3.6 Cell-Selectivity of Ypep-fusion Proteins

Given the role multivalency plays in the potency of Ypep-dependent delivery, we hypothesized that those same effects may contribute to cell-selectivity as well. The delivery of Ypep-GFP, Ypep-GFP-Ypep, and $(Ypep)_5$-phage in PC-3 human prostate cancer cells (PSMA-neg), LNCaP human prostate cancer cells (PSMA-pos), HEK-293T human embryonic kidney cells, MRC-9 human lung fibroblast cells, and Hs 697.Sp human spleen fibroblast cells was compared. The potency and cell-selectivity of Ypep-GFP and Ypep-GFP-Ypep delivery was measured by flow cytometry. Phage titering from cell lysate was used to compare the amount of internalized phage in each cell line.

A single copy of Ypep has appreciable selectivity of delivery (Figure 3.4A). Following treatment with 5 μM Ypep-GFP, we observed ~4-, ~8-, and ~5-fold more internalized GFP in target PC-3 cells compared to off-target LNCaP, HEK-293T, and Hs 687.Sp cells, respectively. However, high levels of GFP fluorescence were also present in off-target MRC-9 cells; only ~1.4-fold more fluorescence was observed in target PC-3 cells. These data suggest that monomeric Ypep is moderately selective for PC-3 cells. We next compared the cell-selectivity of Ypep-GFP-Ypep in the same cell lines mentioned previously. Figure 3.4B shows higher cell-selectivity of GFP uptake in PC-3

cells treated with bivalent Ypep-GFP-Ypep when compared to monomer Ypep-GFP. Like Ypep-GFP, Ypep-GFP-Ypep was taken up by targeted PC-3 cells with much lower levels of internalized GFP detected in off-target LNCaP, HEK-293T, and Hs 697.Sp cells.

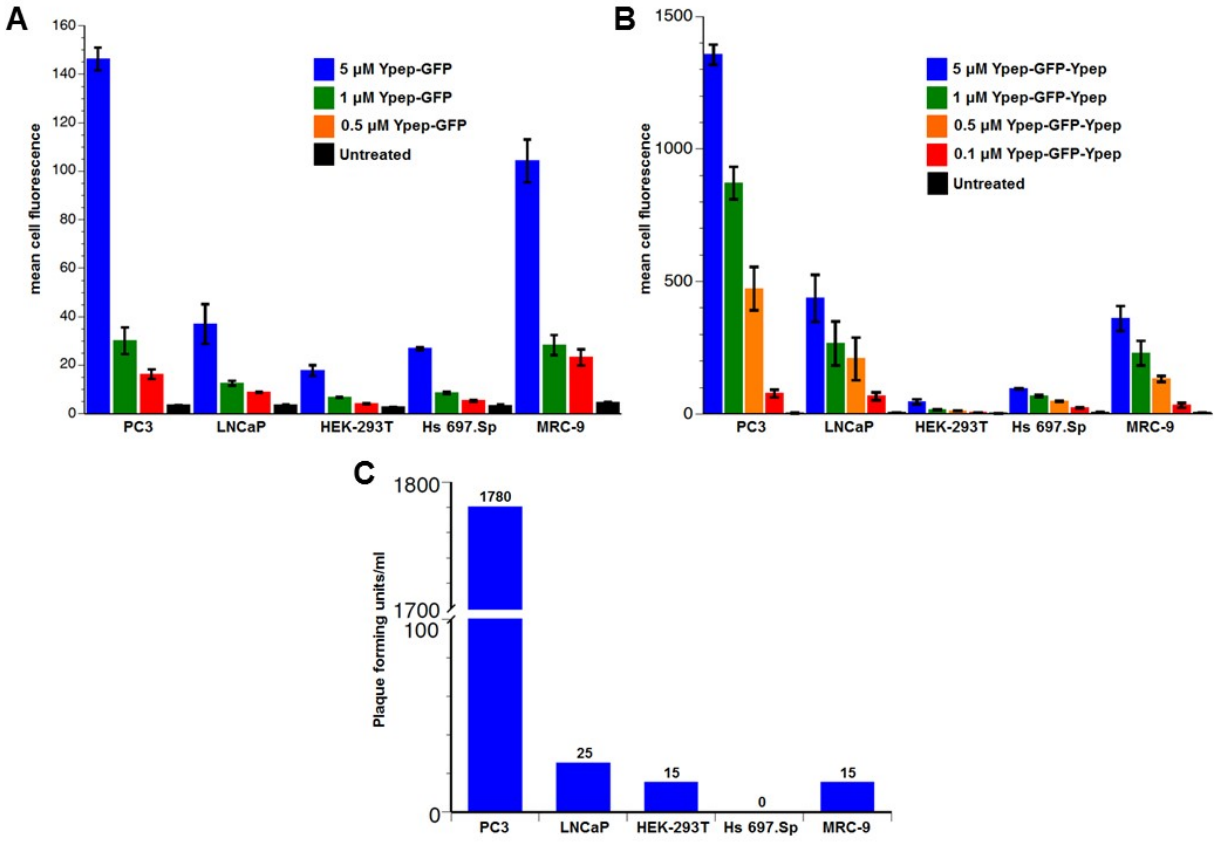

Figure 3.4. The cell selectivity of Ypep fusion proteins and phage. (A) Amounts of internalized GFP in PC-3, LNCaP, HEK293T, Hs 697.Sp, and MRC-9 after treatment with 0.5, 1, or 5 μM Ypep-GFP (B) Amounts of internalized GFP in PC-3, LNCaP, HEK-293T, Hs 697.Sp, and MRC-9 after treatment with 0.1, 0.5, 1, or 5 μM Ypep-GFP-Ypep. (C) Representative phage plaque forming units per milliliter (pfu/mL) generated from the cell lysate of each cell line tested after treatment with 1×10^9 pfu/mL $(Ypep)_5$-phage. Values and error bars in A & B represent the mean and standard deviation of three independent experiments.

However, unlike Ypep-GFP, which was taken up well in both target PC-3 and off-target MRC-9 cells, Ypep-GFP-Ypep showed a ~4-fold preference for PC-3 cells over MRC-9

cells. Taken together, these data demonstrate an important role for multivalency in the cell-selectivity of delivery.

Finally, we tested the cell-selectivity of $(Ypep)_5$-phage delivery by comparing the plaque forming assay results from each of the lysates after incubation with each cell line and washing steps. Cells were treated with 5 mLmL of F12K/10% FBS containing 1.0×10^9 plaque forming units (pfu)/mLmL of $(Ypep)_5$- phage. This equates to a solution with a concentration of 1.7 pM phage. Thus, cell-penetration at this concentration indicates very high potency. After incubation with phage, cells were washed to remove cell-surface-bound phage, and cells were lysed as previously described. In addition to titering the cell lysate, aliquots from each final wash solution were titered to ensure that all surface-bound phage were completely removed before cell lysis. No phage were found in any of the final washing solutions (Experimental Methods). In contrast, high levels of $(Ypep)_5$-phage was found in the PC-3 cell lysate (Figure 3.4C). However, unlike the previously described protein fusions, appreciable levels (>25pfu/mL) of $(Ypep)_5$-phage were not observed in any off-target cell lines. In contrast, >1,500 pfu/mL were observed in *E. coli* treated with PC-3 cell lysate. This represents a drastic change in the cell-selectivity of Ypep-dependent delivery.

Although these data suggest that multivalency effects likely play a role in the cell-selectivity of uptake, the architecture of Ypep display in the context of fusion to

GFP and fusion to the N-terminus of phage coat protein p3 differ greatly. We cannot dismiss the possibility that these architectural changes may play an important role in the cell-selectivity profiles we observe. Nonetheless, the cell-selectivity and potency profiles displayed by bivalent Ypep-GFP fusions and $(Ypep)_5$-phage make Ypep well suited for targeted bioimaging applications, as well as phage-based approaches to biomedical science.

3.7 Mechanism of Ypep Internalization

Studies regarding the mechanism of CPP entry into cells have led to varied results. As discussed in Chapter 1, the way a CPP enters a cell appears to depend on several factors, including CPP sequence[23], charge[24], attached cargo[25,26], and targeted cell type[27]. Unlike most other known CPPs, which often have a high positive charge, Ypep has a theoretical net charge of +1, raising the question of whether or not its mechanism of entry is severely different from those previously studied. Additionally, data showed that multivalency functioned to further increase internalization of the constructs. Given this information, we worked to characterize the method of internalization.

The first tests performed compared internalization at 37 °C and 4 °C of 15 μM Ypep-GFP, 10 μM Ypep-GFP-Ypep, and 1×10^9 pfu/mL $(Ypep)_5$-phage (Figures 3.5B, 3.5I, & 3.5P) into confluent PC-3 cells. In the case of all three constructs, internalization was not observed, indicating that cell penetration is energy-dependent, likely through some

form of endocytosis. Next, PC-3 cells were pre-treated with an assortment of small molecule inhibitors that block various pathways of endocytosis. The variant Ypep constructs (with concentrations previously indicated) were incubated with PC-3 cells 10 minutes post-treatment. Results observed for Ypep-GFP were consistent with those seen for Ypep-GFP-Ypep.

In cells treated with 5 μg/mL chlorpromazine (Figures 3.5F & 3.5M) and 10 μg/mL cytochalasin D (Figures 3.5G & 3.5N) no appreciable decrease in fluorescence was observed. These data indicate that internalization was not occurring through either clathrin-mediated endocytosis or receptor-mediated endocytosis[28], respectively. When cells were pre-treated with 400 μg/mL of heparin sulfate, internalization was inhibited for all three Ypep constructs (Figures 3.5D, 3.5K, & 3.5Q). As a polysaccharide often expressed on the surface of mammalian cells, inhibition under these conditions suggest that the Ypep-constructs may interact with cell-surface glycosaminoglycans to facilitate internalization[29]. In addition to these results, cellular uptake was observed to have significantly decreased in the presence of 5 μg/mL of filipin (Figures 3.5C & 3.5J). Filipin is used as an inhibitor for lipid-raft or caveolae-dependent endocytotic pathways[30]. However, upon treatment with 25 mg/mL of nystatin, an inhibitor of caveolae-dependent endocytosis[28], the same results were not observed (Figures 3.5E & 3.5L). Collectively, these results suggest that cargo fused to Ypep enter the cell through some type of lipid raft-mediated endocytosis and that binding to cell-surface

glycosaminoglycans promote the process.

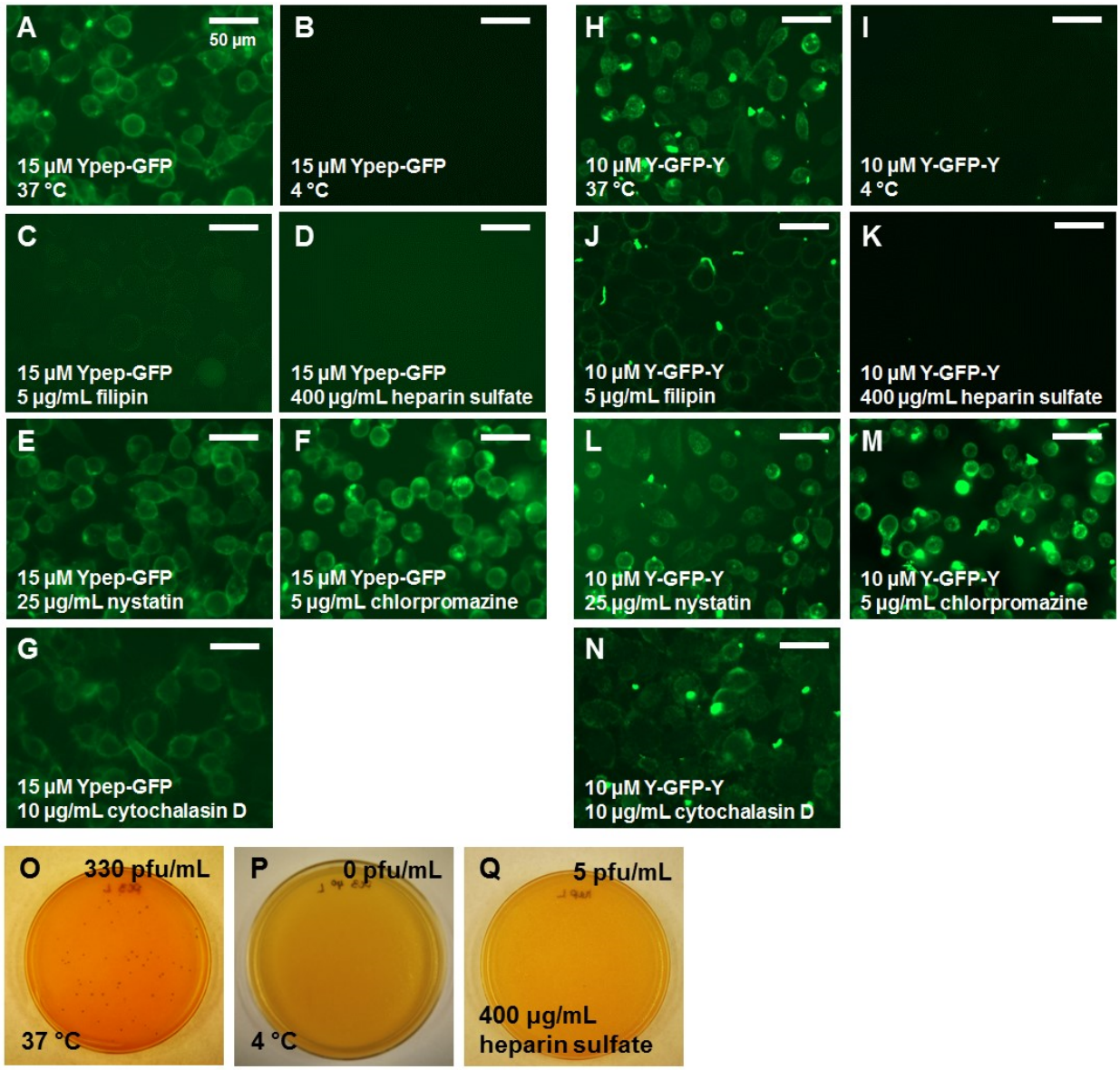

Figure 3.5 Probing the mechanism of internalization. PC-3 cells are treated with: (A) 15 μM Ypep-GFP at 37 °C. (B) 15 μM Ypep-GFP at 4 °C. (C) 15 μM Ypep-GFP and 5μg/mL filipin (D) 15 μM Ypep-GFP and 400 μg/mL heparin sulfate. (E) 15 μM Ypep-GFP and 25 μg/mL nystatin(F) 15 μM Ypep-GFP and 5 μg/mL chlorpromazine(G) 15 μM Ypep-GFP and 10 μg/mL cytochalasin D, a known inhibitor of actin polymerization. (H-N) Cells are treated with 10 μM Ypep-GFP-Ypep and the same small molecule inhibitors as described in figures 3.5A-3.5G. All fluorescence images were obtained with a 200 ms exposure, 20% lamp intensity. Scale bars in each image is 50 μm. Plaque forming assays were performed on PC-3 cells treated with (O) 1×10^9 pfu/mL $(Ypep)_5$-phage at 37 °C. (P) 1×10^9 pfu/mL $(Ypep)_5$-phage at 4 °C. Q) 1×10^9 pfu/mL $(Ypep)_5$-phage and 400 μg/mL heparin sulfate.

Data from experiments with filipin, cytochalasin D, nystatin, and chlorpromazine performed with $(Ypep)_5$-phage could not be properly quantified. As the inhibitors are often toxic to the cells, they were unable to withstand the stringent washing conditions required to thoroughly remove phage from the cell surface.

3.8 Cytotoxicity and Robustness of Ypep-dependent Delivery

To assess the cytotoxicity of Ypep variants under conditions required for appreciable uptake, we performed an MTT (3-[4,5-dimethylthiazol-2-yl]-2,5-diphenyltetrazolium bromide) assay on PC-3 cells after treatment with 0.5, 1, or 5 μM Ypep-GFP or Ypep-GFP-Ypep or 1×10^9 pfu/mL $(Ypep)_5$-phage. As shown in Figure 3.6A-C, no apparent cytotoxicity to PC-3 cells was observed for any of the Ypep variants.

In order for a CPP to be used *in vivo*, it must penetrate the target cell in the presence of a complex solution, such as whole blood. PC-3 cells were treated with either 10 μM Ypep-GFP or Ypep-GFP-Ypep in F12K/10% FBS solution containing 50% whole human blood. Cells were then washed as previously described, and red blood cells were removed using standard methods. Cell fluorescence was measured by flow cytometry. Ypep-GFP-Ypep, but not Ypep-GFP penetrated PC-3 cells in a solution containing human blood (Figure 3.6D & 3.6E). In addition, when PC-3 cells were treated with 1×10^9 pfu/mL $(Ypep)_5$-phage in F12K/10% FBS solution containing 50% whole blood, appreciable levels of phage were found in cell lysate. These data suggest that

multivalent Ypep-dependent cell-penetration is functional in blood and may perhaps be utilized as a potent tool for intracellular delivery or therapeutics and imaging reagents.

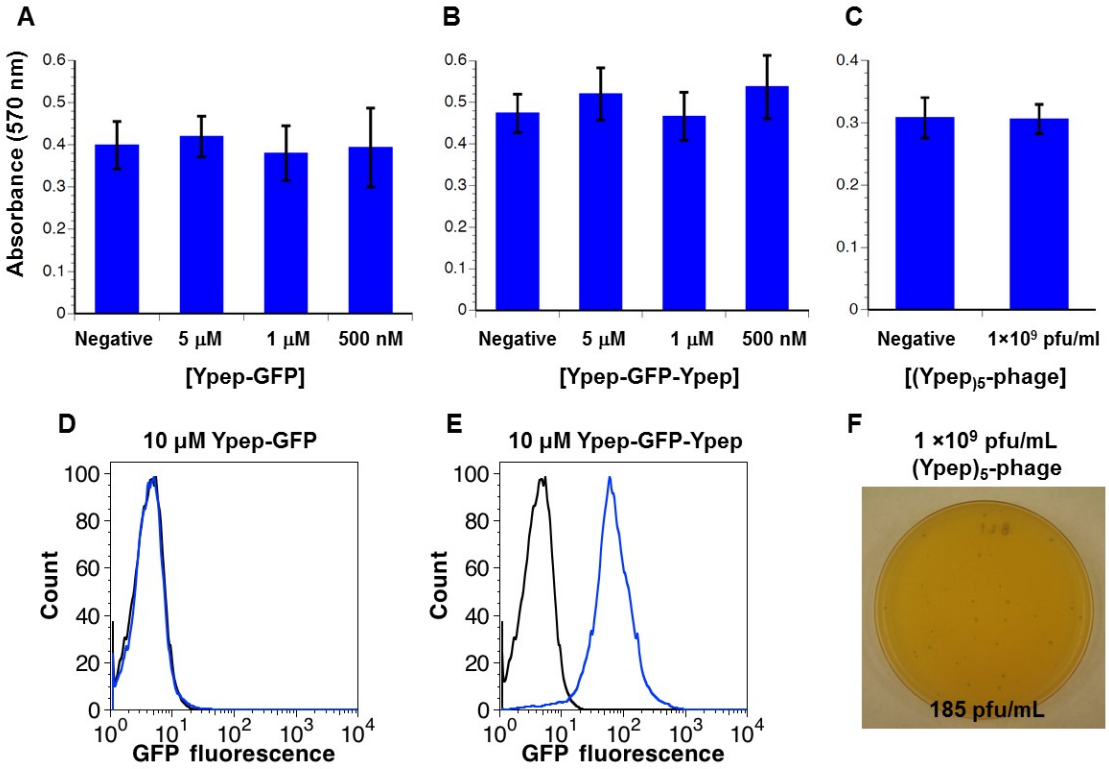

Figure 3.6 Cytotoxicity and delivery in a complex solution. (A-C) MTT assays of PC-3 cells treated with various concentrations of Ypep-GFP, Ypep-GFP-Ypep, or $(Ypep)_5$-phage. Values and error bars represent the mean and standard deviation of three separate experiments. (D-E) GFP uptake of 10 μM Ypep-GFP and Ypep-GFP-Ypep after incubation with PC-3 in whole blood and F12K/10% FBS. (F) Plaque forming assay of PC-3 cells treated with 1×10^9 pfu/mL $(Ypep)_5$-phage in whole blood and F12K/10% FBS.

3.9 Conclusion

Using phage display, we identified a novel CPP (Ypep) whose potency and selectivity for targeted PC-3 prostate cancer cells is tightly controlled through multivalency. A single copy of Ypep displayed the N-terminus of GFP (Ypep-GFP) penetrates various human cells with modest potency and poor selectivity. The addition

of a second copy of Ypep attached to the C-terminus of GFP (Ypep-GFP-Ypep), enhanced potency by ~9- to ~29-fold over the same set of human cells as well as cell-selectivity for PC-3 cells. With five copies of Ypep displayed on the p3 coat protein of phage ($(Ypep)_5$-phage) PC-3 cellular uptake was potent with great selectivity. Collectively, our results reveal Ypep as a CPP capable of delivering protein (GFP) or nanometer-sized cargo (phage). Both Ypep-GFP-Ypep and $(Ypep)_5$-phage penetrate cells in the presence of human blood. All Ypep variants are non-cytotoxic and both Ypep-GFP and Ypep-GFP-Ypep penetrate PC-3 cells through a caveolae-independent lipid-raft mediated endocytosis.

3.10 Experimental Methods

Materials

PBS, 0.25% trypsin, Dulbecco's modified Eagle's medium (DMEM), RPMI-1640 medium, B-PER Bacterial Protein Extraction Reagent, Modified Lowry Protein Assay Kit, and Pierce Firefly Luciferase Glow Assay Kit were purchased from Thermo Scientific (Waltham, MA, USA). Cellgro F-12K medium was purchased from MediaTech (Manassas, VA, USA). Fetal bovine serum (FBS) was purchased from PAA Laboratories (Westborough, MA, USA). cOmplete Mini Protease Inhibitor Cocktail Tablets were purchased from Roche (Indianapolis, IN, USA). TACS MTT reagent was purchased from

Trevigen (Gaithersburg, MD, USA). The Ph.D.-12 Phage Display Library, Nco I HF, and KpnI HF were purchased from New England Biolabs (NEB) (Ipswich, MA, USA). Sodium deoxycholate, heparin sulfate, and imidazole were purchased from Sigma-Aldrich (St. Louis). Ni-NTA agarose resin was purchased from QIAGEN (Hilden, Germany). Lowry protein assay was purchased from Pierce Biotechnology (Rockford, IL, USA). Human blood was purchased from Innovative Research (Novi, MI, USA).

Instrumentation

Fluorescence microscopy images were taken on an EVOS fluorescence inverted microscope from the Advanced Microscopy Group (AMG). MTT assay readings were taken on a Synergy Mx microplate reader from BioTek Instruments (Winooski, VT, USA). Flow cytometry experiments were performed on a MoFlo (Dako Colorado, Fort Collins, CO, USA) flow cytometer using a solid-state iCyt 488 nm (blue) laser to measure GFP fluorescence.

Mammalian Cell Culture

Human prostate adenocarcinoma cells (PC-3) cells were cultured in F12K with 10% fetal bovine serum (FBS). Human prostate carcinoma cells (LNCaP) and human embryonic lung fibroblasts (MRC-9) cells were cultured in RPMI-1640 media with 10% FBS; human spleen fibroblasts (Hs 697.Sp) and HEK293T cells were cultured in high glucose Dulbecco's modified Eagle's medium (DMEM) with 10% fetal bovine serum (FBS). PC-3, LNCaP, and MRC-9 cells were incubated at 37 °C with 5% CO_2 environment. Hs

697.Sp cells were incubated at 37 °C with 10% CO_2 environment. All cells were obtained from the American Type Culture Collection.

Phage Selection

Positive Selection: A 10 mL solution of F12K/10% FBS containing 531010 phage library members (Ph.D.-12 Phage Display Library, NEB) was added to 80% confluent PC-3 cells grown as a monolayer in a T25 culture flask and incubated at 37 °C under 5% CO2 environment for 3 hours. After incubation, cells were then placed on ice for 5 minutes and washed with 4 °C PBS five times while on ice. Cells were then washed three times with 4 °C Tris-buffered saline (TBS)/0.1% v/v Tween-20 for 3 minutes each while on ice. The remaining surface-bound phage was proteolyzed by addition of a 5 mL TBS/subtilisin (3 mg/mL) for 45 minutes at 4 °C. Cells were then transferred into a 15 mL plastic tube and pelleted for 5 minutes at 3,000 rpm and at 4 °C. Supernatant was removed and cells were resuspended in 5 mL PBS/5 mL protease inhibitor for 15 minutes at 4 °C and then pelleted for 5 min at 3,000 rpm and 4 °C. Supernatant was removed, and cells were resuspended in 1 mL of PBS and pelleted for 5 min at 3,000 rpm and 4 °C. Supernatant was removed and saved as the last wash solution for subsequent titering. Cells were lysed with 0.5 mL of lysis buffer (2% sodium deoxycholate, 10 mM Tris-HCl, and 2 mM EDTA) and 0.5 mL of TBS for 1 hour at room temperature. After cell lysis, internalized phage was amplified in a 150 mL flask containing 30 mL LB, 360 mL 0.1 M $CaCl_2$,20 mg/mL tetracycline, and 0.15 mL of E. coli

(ER2837) that had been grown to optical density (OD) ~0.5. The final wash solution (200 mL) or the cell lysate was then added, and this solution was incubated at 37 °C, 250 rpm for 5 hour. E. coli was pelleted for 10 minutes at 10,000 rpm and 4 °C. Supernatant containing phage was transferred to another tube, and E. coli cell debris was pelleted at 10,000 rpm for 10 minutes at 4 °C. Phage from the supernatant was precipitated by addition of 5 mL 20% PEG-8000/2.5 M NaCl. Phage was only amplified after positive selection rounds; the phage-containing media from negative selections was directly added to positive cell lines without amplification of the phage.

Negative selection: A 10 mL solution containing 1×10^9 pfu/mL amplified from the positive selection was added to a T25 culture flask and incubated at 37 C with 5% CO2 environment for 1 hour. Rounds of positive and negative selection were performed three times.

Plasmid Construction

All constructs were cloned into pET plasmids. DNAs encoding cell-penetrating peptide fusions with sfGFP were assembled using oligonucleotide overlap gene construction and PCR.

Protein purification

BL21-DE3 E. coli were grown in 500 mL LB cultures at 37 °C to OD_{600} ~0.6 and induced with 1mM IPTG at 30 °C overnight. Cells were then pelleted by centrifugation and lysed with 25 mL B-PER. Cell lysate was cleared by centrifugation (17,000 rpm, 30

minutes), and supernatant was mixed with 1 mL of Ni-NTA agarose resin for 1 hour at 4 °C under agitation. Resin was collected by centrifugation (4,950 rpm, 10 minutes). Ni-NTA agarose resin was washed with 50 mL of PBS containing 300 mM NaCl pH 8.0 and then 50 mL of PBS containing 300 mM NaCl and 20 mM imidazole. Protein was then eluted with 5 mL PBS containing 300 mM NaCl and 500 mM imidazole. Eluted protein was dialyzed against PBS and analyzed for purity by SDS-PAGE followed by staining with Coomassie Blue. Protein concentrations were measured using a modified Lowry Protein Assay Kit.

Flow Cytometry

Mammalian cells were grown to ~80% confluency in a 6-well plate. Cells were washed once with PBS and PBS containing Ypep-GFP, (Ypep)2-GFP, or Ypep-GFP-Ypep was added. Cells were incubated with each PBS/protein solution for 3 hours at 37 °C under 5% CO_2 environment, then washed twice with PBS, and three times with PBS-HS (heparin sulfate 20 U/mL) for 10 minutes each at 37 °C. Cells were then removed from the tissue culture plate by addition of 0.5 mL of 0.25% trypsin and pelleted by centrifugation. Cell pellet was resuspended in PBS/10% FBS, and cell fluorescence was analyzed by flow cytometry.

Mechanism of Cell Penetration

PC-3 cells were grown to ~80% confluency in a 12-well tissue culture plate. Cells were then washed once with PBS and incubated with the small molecule inhibitor in PBS for

10 minutes at 37 °C under 5% CO_2 environment. The PBS-small molecule solution was then removed, and a PBS solution containing either 15 mM Ypep-GFP or 10 mM Ypep-GFP-Ypep with a small molecule inhibitor in PBS was added to the cells. Cells were incubated in each solution for 30 minutes at 37 °C under 5% CO_2 environment. Cells were washed twice with PBS, once with PBS-HS (heparin sulfate 20 U/mL), and imaged on an EVOS fl fluorescence.

Cell-Selectivity Experiments

For experiments involving Ypep-GFP and Ypep-GFP-Ypep, cell penetration was measured using flow cytometry, as described above (see Flow Cytometry). For cell selectivity experiments involving $(Ypep)_5$-phage, cells were grown to ~80% confluency and then treated with 5 mL of media supplemented with 10% FBS and 1×10^9 pfu/mL $(Ypep)_5$-phage for 3 hours at 37 °C and 5% CO2 environment. Cells were washed and lysed as previously described (see Phage Selection). An aliquot of the final wash solution was kept for titering. Following cell lysis (see Phage Selection), aliquots from cell lysate and the last wash before lysis were titered. Titering was carried out as described above (see Phage Selection). After this time, the entire E. coli mixture was plated on IPTG/X-gal LB-agar plates and incubated at 37 °C for 18 hours.

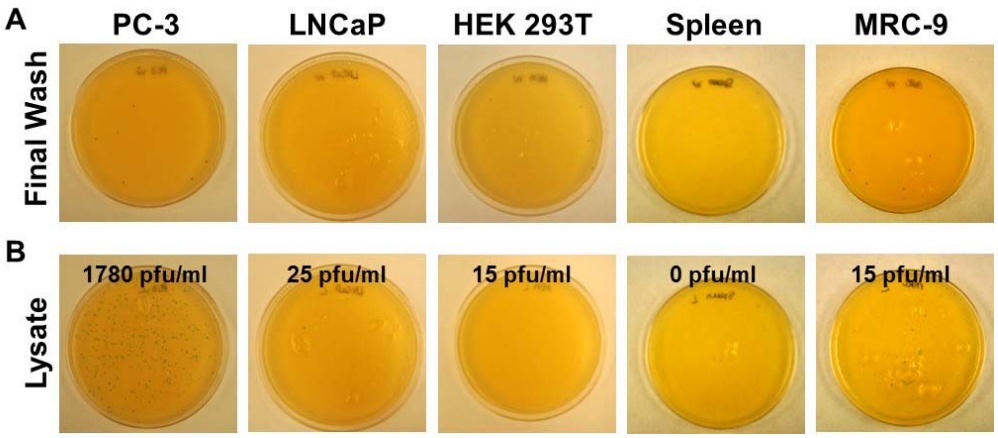

Figure 3.7 Plaque forming assay data. Phage plaque-forming units generated from (A) aliquots from the final wash solution of each cell line tested following incubation with *E. coli* for 5 minutes at 37 °C then grown on an IPTG/x-gal plate for 18 hours (B) Aliquots of cell lysate of each cell line tested, following the same incubation. Phage express β-galactosidase, thus phage present on each plate are seen as blue plaques.

MTT Cell Viability Assay

Assays were performed following the provided instructions. PC-3 cells were grown to ~80% confluency in a 12-well tissue culture plate. Cells were then washed once with PBS and incubated with 0.5–5 mM solutions of Ypep-GFP or Ypep-GFP-Ypep in PBS for 3 hours at 37 °C under a 5% CO_2 environment. Cells were washed three times with PBS-HS (20 U/mL heparin sulfate) and then incubated with 0.5 mL media containing 25 mL of MTT reagent for 4.5 hours. After such time, a 250 mL detergent reagent was added to the cells, and they were incubated for an additional 30 minutes at 37 °C under a 5% CO_2 environment. Absorbance was measured at 570 nm on a Synergy Mx microplate reader. Cell viability of cells treated with $(Ypep)_5$-phage was determined after a 3 hours incubation with 5 mL of 1×10^9 pfu/mL Ypep-phage (1.67 pM) in F12K medium

supplemented with 10% FBS at 37 °C under a 5% CO_2 environment. PC-3 cells were washed twice with PBS, and the MTT assay was performed as described above.

Ypep-GFP and Ypep-GFP-Ypep Internalization in the Presence of Human Blood

PC-3 cells were grown to ~80% confluency in a 6-well plate. Whole blood was diluted in half with F12K/10% FBS. To this solution either Ypep-GFP or Ypep- GFP-Ypep was added to final concentrations of 10 mM. Cells were incubated with these solutions for 1 hour, washed once with PBS, and then washed twice with a red blood cell lysis buffer (0.15 M NH_4Cl, 0.01 M $KHCO_3$, and 0.0001 M EDTA [pH = 7.7]) to remove all red blood cells. Cells were washed three times with PBS-HS (20 U/mL heparin sulfate) and imaged on an EVOS fl fluorescence microscope.

$(Ypep)_5$-Phage Internalization in the Presence of Human Blood

PC-3 cells were grown to ~80% confluency in a 6-well plate. Whole blood was diluted in half with F12K/10% FBS. To this solution, 1×10^9 $(Ypep)_5$-phage (1.67 pM) was added. Cells were incubated in this solution for 3 hr at 37 C under a 5% CO_2 environment. Cells were washed twice with red blood cell lysis buffer, twice with PBS, and three times with Tris-buffered saline (TBS)/ 0.1% v/v Tween-20 for 3 minutes each on ice. Cells were then washed as described. Aliquots from final wash and cell lysate solutions were titered as described previously (see Phage Selection: Positive Selection).

Sequence Information

GFP

MGGASKGEELFTGVVPILVELDGDVNGHKFSVRGEGEGDATNGKLTLKFICTTGKLP
VPWPTLVTTLTYGVQCFSRYPDHMKQHDFFKSAMPEGYVQERTISFKDDGTYKTRAE
VKFEGDTLVNRIELKGIDFKEDGNILGHKLEYNFNSHNVYITADKQKNGIKANFKIR
HNVEDGSVQLADHYQQNTPIGDGPVLLPDNHYLSTQSALSKDPNEKRDHMVLLEF
VTAAGITHGMDELYKHHHHHH

Ypep-GFP

MGYTFGLKTSFNVQGGSGGSGGSGGSMGGASKGEELFTGVVPILVELDGDVNGHKF
SVRGEGEGDATNGKLTLKFICTTGKLPVPWPTLVTTLTYGVQCFSRYPDHMKQHDFF
KSAMPEGYVQERTISFKDDGTYKTRAEVKFEGDTLVNRIELKGIDFKEDGNILGHKLE
YNFNSHNVYITADKQKNGIKANFKIRHNVEDGSVQLADHYQQNTPIGDGPVLLPDN
HYLSTQSALSKDPNEKRDHMVLLEFVTAARITHGMDELYKHHHHHH

Tat-GFP

MGYGRKKRRQRRRGGSGGSGGSGGSMGGASKGEELFTGVVPILVELDGDVNGHKFS
VRGEGEGDATNGKLTLKFICTTGKLPVPWPTLVTTLTYGVQCFSRYPDHMKQHDFFK
SAMPEGYVQERTISFKDDGTYKTRAEVKFEGDTLVNRIELKGIDFKEDGNILGHKLEY
NFNSHNVYITADKQKNGIKANFKIRHNVEDGSVQLADHYQQNTPIGDGPVLLPDN
HYLSTPSALSKDPNEKRDHMVLLEFVTAAGITHGMDELYKHHHHHH

Pen-GFP

MGRQIKIWFQNRRMKWKKGGSGGSGGSGGSMGGASKGEELFTGVVPILVELDGDV
NGHKFSVRGEGEGDATNGKLTLKFICTTGKLPVPWPTLVTTLTYGVQCFSRYPDHMK
QHDFFKSAMPEGYVQERTISFKDDGTYKTRAEVKFEGDTLVNRIELKGIDFKEDGNIL
GHKLEYNFNSHNVYITADKQKNGIKANFKIRHNVEDGSVQLADHYQQNTPIGDGP
VLLPDNHYLSTQSALSKDPNEKRDHMVLLEFVTAAGITHGMDELYKHHHHHH

Ypep-GFP-Ypep

MGYTFGLKTSFNVQGGSGGSGGSGGSMGGASKGEELFTGVVPILVELDGDVNGHKF
SVRGEGEGDATNGKLTLKFICTTGKLPVPWPTLVTTLTYGVQCFSRYPDHMKQHDFF
KSAMPEGYVQERTISFKDDGTYKTRAEVKFEGDTLVNRIELKGIDFKEDGNILGHKLE
YNFNSHNVYITADKQKNGIKANFKIRHNVEDGSVQLADHYQQNTPIGDGPVLLPDN

HYLSTQSALSKDPNEKRDHMVLLEFVTAAGITHGMDELYKHHHHHHGGSGGSGGS
MYTFGLKTSFNVQ

Pen-GFP-Pen

MGRQIKIWFQNRRMKWKKGGSGGSGGSGGSMGGASKGEELFTGVVPILVELDGDV
NGHKFSVRGEGEGDATNGKLTLKFICTTGKLPVPWPTLVTTLTYGVQCFSRYPDHMK
QHDFFKSAMPEGYVQERTISFKDDGTYKTRAEVKFEGDTLVNRIELKGIDFKEDGNIL
GHKLEYNFNSHNVYITADKQKNGIKANFKIRHNVEDGSVQLADHYQQNTPIGDGP
VLLPDNHYLSTQSALSKDPNEKRDHMVLLEFVTAAGITHGMDELYKHHHHHHGGS
GGSGGSMRQIKIWFQNRRMK

Tat-GFP-Tat

MGYGRKKRRQRRRGGSGGSGGSGGSMGGASKGEELFTGVVPILVELDGDVNGHKFS
VRGEGEGDATNGKLTLKFICTTGKLPVPWPTLVTTLTYGVQCFSRYPDHMKQHDFFK
SAMPEGYVQERTISFKDDGTYKTRAEVKFEGDTLVNRIELKGIDFKEDGNILGHKLEY
NFNSHNVYITADKQKNGIKANFKIRHNVEDGSVQLADHYQQNTPIGDGPVLLPDN
HYLSTQSALSKDPNEKRDHMVLLEFVTAAGITHGMDELYKHHHHHHGGSGGSGGS
MYGRKKRRQRRR

Ypep$_2$-GFP

MGYTFGLKTSFNVQGGSGGSGGSGGSYTFGLKTSFNVQGGSGGSGGSGGSMGGASK
GEELFTGVVPILVELDGDVNGHKFSVRGEGEGDATNGKLTLKFICTTGKLPVPWPTL
VTTLTYGVQCFSRYPDHMKQHDFFKSAMPEGYVQERTISFKDDGTYKTRAEVKFEGD
TLVNRIELKGIDFKEDGNILGHKLEYNFNSHNVYITADKQKNGIKANFKIRHNVEDG
SVQLADHYQQNTPIGDGPVLLPDNHYLSTQSALSKDPNEKRDHMVLLEFVTAAGIT
HGMDELYKHHHHHH

REFERENCES

(1) Trover, J. K., Beckett, M. Lou, and Wright, G. L. (1995) Detection and characterization of the prostate-specific membrane antigen (PSMA) in tissue extracts and body fluids. *Int. J. Cancer 62*, 552–558.

(2) Ghosh, A., and Heston, W. D. W. (2004) Tumor target prostate specific membrane antigen (PSMA) and its regulation in prostate cancer. *J. Cell. Biochem. 91*, 528–39.

(3) Chang, S. S., Reuter, V. E., and Heston, W. D. W. (1999) Five Different Anti-Prostate-specific Membrane Antigen (PSMA) Antibodies Confirm PSMA Expression in Tumor-associated Neovasculature Five Different Anti-Prostate-specific Membrane Antigen (PSMA) Antibodies 3192–3198.

(4) Veldhoen, S., Laufer, S. D., Trampe, A., and Restle, T. (2006) Cellular delivery of small interfering RNA by a non-covalently attached cell-penetrating peptide: quantitative analysis of uptake and biological effect. *Nucleic Acids Res. 34*, 6561–73.

(5) Koren, E., and Torchilin, V. P. (2012) Cell-penetrating peptides: Breaking through to the other side. *Trends Mol. Med. 18*, 385–393.

(6) Frankel, A. D., and Pabo, C. O. (1988) Cellular uptake of the tat protein from human immunodeficiency virus. *Cell 55*, 1189–1193.

(7) Derossi, D., Chassaing, G., and Prochiantz, A. (1998) Trojan peptides: the penetratin system for intracellular delivery. *Trends Cell Biol. 8*, 84–87.

(8) Oehlke, J., Scheller, A., Wiesner, B., Krause, E., Beyermann, M., Klauschenz, E., Melzig, M., and Bienert, M. (1998) Cellular uptake of an alpha-helical amphipathic model peptide with the potential to deliver polar compounds into the cell interior non-endocytically. *Biochim. Biophys. Acta 1414*, 127–139.

(9) Milletti, F. (2012) Cell-penetrating peptides: classes, origin, and current landscape. *Drug Discov. Today 17*, 850–60.

(10) Wyman, T. B., Nicol, F., Zelphati, O., Scaria, P. V, Plank, C., and Szoka, F. C. (1997) Design, synthesis, and characterization of a cationic peptide that binds to nucleic acids and permeabilizes bilayers. *Biochemistry 36*, 3008–3017.

(11) Ueberberg, S., and Schneider, S. (2010) Phage library-screening: A powerful approach for generation of targeting-agents specific for normal pancreatic islet-cells and islet-cell carcinoma in vivo. *Regul. Pept. 160*, 1–8.

(12) Watkins, N. a, and Ouwehand, W. H. (2000) Introduction to antibody engineering and phage display. *Vox Sang. 78*, 72–79.

(13) Ronca, R., Benzoni, P., De Luca, A., Crescini, E., and Dell'Era, P. (2012) Phage Displayed Peptides/Antibodies Recognizing Growth Factors and Their Tyrosine Kinase Receptors as Tools for Anti-Cancer Therapeutics. *Int. J. Mol. Sci. 13*, 5254–5277.

(14) Chonn, a, and Cullis, P. R. (1995) Recent advances in liposomal drug-delivery systems. *Curr. Opin. Biotechnol. 6*, 698–708.

(15) Hughes, B. (2010) Antibody-drug conjugates for cancer: poised to deliver? *Nat. Rev. Drug Discov. 9*, 665–7.

(16) Cronican, J. J., Thompson, D. B., Beier, K. T., McNaughton, B. R., Cepko, C. L., and Liu, D. R. (2010) Potent delivery of functional proteins into Mammalian cells in vitro and in vivo using a supercharged protein. *ACS Chem. Biol. 5*, 747–52.

(17) Cronican, J. J., Beier, K. T., Davis, T. N., Tseng, J.-C., Li, W., Thompson, D. B., Shih, A. F., May, E. M., Cepko, C. L., Kung, A. L., Zhou, Q., and Liu, D. R. (2011) A class of human proteins that deliver functional proteins into mammalian cells in vitro and in vivo. *Chem. Biol. 18*, 833–8.

(18) McNaughton, B. R., Cronican, J. J., Thompson, D. B., and Liu, D. R. (2009) Mammalian cell penetration, siRNA transfection, and DNA transfection by supercharged proteins. *Proc. Natl. Acad. Sci. U. S. A. 106*, 6111–6.

(19) Meade, B. R., and Dowdy, S. F. (2008) Enhancing the cellular uptake of siRNA duplexes following noncovalent packaging with protein transduction domain peptides. *Adv. Drug Deliv. Rev. 60*, 530–6.

(20) Mammen, M., Choi, S.-K., and Whitesides, G. M. (1998) Polyvalent Interactions in Biological Systems: Implications for Design and Use of Multivalent Ligands and Inhibitors. *Angew. Chemie Int. Ed. 37*, 2754–2794.

(21) Moss, J. A., Lillo, A., Kim, Y. S., Gao, C., Ditzel, H., and Janda, K. D. (2005) A dimerization "switch" in the internalization mechanism of a cell-penetrating peptide. *J. Am. Chem. Soc. 127*, 538–9.

(22) Tseng, Y.-L., Liu, J.-J., and Hong, R.-L. (2002) Translocation of liposomes into cancer cells by cell-penetrating peptides penetratin and tat: a kinetic and efficacy study. *Mol. Pharmacol. 62*, 864–72.

(23) Langel, Ü. (Ed.). (2002) Cell-Penetrating peptides: Processes and Applications 1st ed., p 406. CRC Press, Boca Raton.

(24) Lundberg, P., and Langel, Ü. (2003) A brief introduction to cell-penetrating peptides. *J. Mol. Recognit. 16*, 227–233.

(25) Wadia, J. S., Stan, R. V, and Dowdy, S. F. (2004) Transducible TAT-HA fusogenic peptide enhances escape of TAT-fusion proteins after lipid raft macropinocytosis. *Nat. Med. 10*, 310–315.

(26) Rothbard, J. B., Jessop, T. C., and Wender, P. a. (2005) Adaptive translocation: the role of hydrogen bonding and membrane potential in the uptake of guanidinium-rich transporters into cells. *Adv. Drug Deliv. Rev. 57*, 495–504.

(27) Deshayes, S., Morris, M. C., Divita, G., and Heitz, F. (2005) Cell-penetrating peptides: tools for intracellular delivery of therapeutics. *Cell. Mol. life Sci. 62*, 1839–1849.

(28) Ivanov, A. I. (2008) Pharmacological inhibition of endocytic pathways: is it specific enough to be useful? *Methods Mol. Biol. 440*, 15–33.

(29) Tyagi, M., Rusnati, M., Presta, M., and Giacca, M. (2001) Internalization of HIV-1 tat requires cell surface heparan sulfate proteoglycans. *J. Biol. Chem. 276*, 3254–61.

(30) Schnitzer, J. E., Oh, P., Pinney, E., and Allard, J. (1994) Filipin-sensitive caveolae-mediated transport in endothelium: reduced transcytosis, scavenger endocytosis, and capillary permeability of select macromolecules. *J. Cell Biol. 127*, 1217–32.

CHAPTER FOUR

CELL-PENETRATING PEPTIDE MUTAGENESIS FACILITATES INCREASED DELIVERY EFFICIENCY AND CELL-SELECTIVITY

4.1 Introduction

Previously, we described our efforts to develop a cell-selective, cell-penetrating peptide capable of delivering reagents and proteins to PC-3 prostate cancer cells[1]. This chapter will focus on the efforts to further enhance potency and selectivity of said CPP and show its ability to deliver functional enzymes as well as fluorescent proteins to mammalian cells.

4.2 Alanine Scanning Determines the Role of Each Residue in Ypep

A library of Ypep alanine mutants fused to sfGFP were produced in order to identify which residues were necessary for protein uptake and which could be mutated to enhance delivery and selectivity. Each mutant peptide was fused to GFP with a $(GGS)_4$ linker. Cultured PC-3 cells were incubated with 5 μM solutions of each Ypep-GFP mutant, washed twice with PBS, washed an additional three times with PBS Heparin Sulfate (20 U/mL), trypsinized from the cell-culture plate, and GFP uptake quantitated through flow cytometry. The majority of mutations resulted in significantly decreased or abolished GFP uptake. A number of commonly used CPPs such as Tat,

polyarginine and penetratin are polycationic, and rely on high-theoretical net charge for cell uptake[2–5]. In contrast, Ypep has a theoretical net change of +1. Interestingly, mutating the single positively charged residue (Lys6) to alanine decreased GFP uptake ~4-fold (Figure 4.1B).

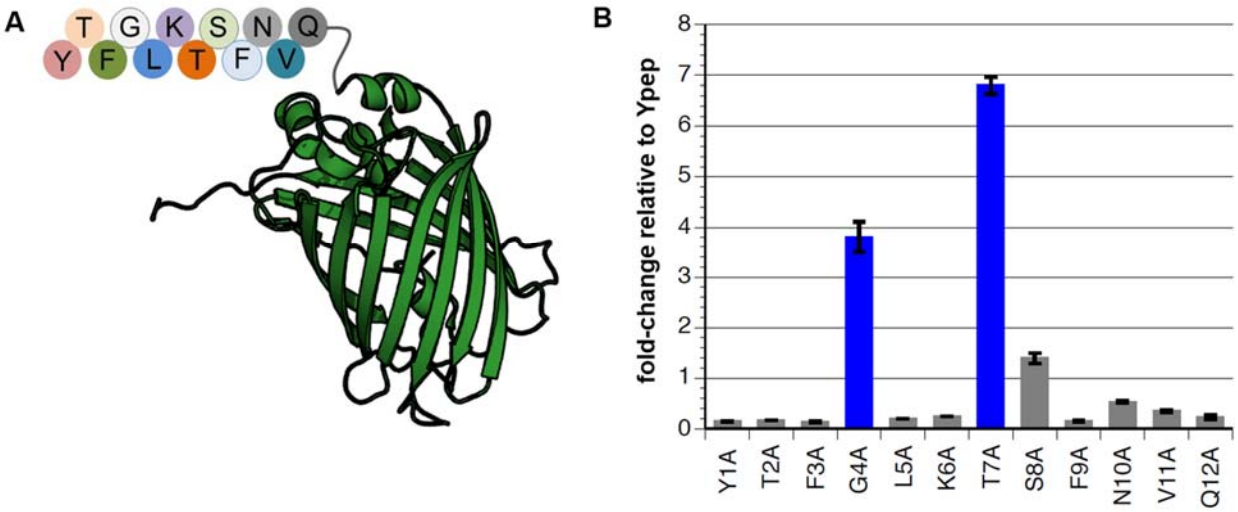

Figure 4.1 Alanine scan of Ypep fusion protein. (A) Native amino acid sequence of Ypep displayed on the N-terminus of GFP. (B) Fold-change in GFP uptake for alanine mutants of Ypep-GFP, relative to Ypep-GFP. PC-3 cells were treated with 5 μM solutions of mutant Ypep-GFP, then washed to remove cell surface-bound protein. GFP uptake was quantitated by flow cytometry. Values and error bars represent the mean and standard deviation of three independent experiments.

Ser8Ala showed a slight increase in deliver, but two mutations Gly4Ala and Thr7Ala showed marked increase in delivery (Fig 4.1B). Gly4Ala and Thr7Ala mutations delivered ~3.8- and ~6.8-fold more GFP to PC-3 cells compared to native Ypep, respectively. Based on these results, further mutations to Gly4 and Thr7 were prepared.

4.3 Optimizing Cellular Uptake of Ypep

A library of Ypep mutants containing either negatively charged (aspartic acid), positively charged (lysine), aromatic (phenylalanine), hydrogen bond donated (serine), or amide (asparagine) functional groups at positions 4 or 7 were expressed as N-terminal fusions to GFP. Their uptake efficiencies were determined through previously established methods. Compared to uptake observed with native Ypep-GFP, the Gly4Asp mutant nearly abolished uptake, and Gly4Phe and Gly4Ser mutants achieved only slightly higher uptake (Fig 4.2A). However, Gly4Lys and Gly4Asn mutants delivered ~3.2 and ~19.2-fold more GFP to PC-3 cells, respectively, compared to native Ypep-GFP. Interestingly, small structural changes at position 4 significantly lowered uptake. While the Gly4Gln mutant was ~6.6-fold improved over Ypep, it was ~2.8-fold less efficient than the Gly4Asn mutant. While the cell surface receptor of Ypep and Ypep mutants has not yet been elucidated, the fact that the addition of a methylene unit significantly lowers uptake supports a model wherein a well-defined interaction between Ypep(G4N)-GFP and a cell-surface receptor is required for efficient uptake. Further, the interaction is not only a function of the sequence-defined amide group display on the CPP, but also the spatial orientation of that group.

The same mutations were performed at residue 7. The Thr7Asp mutant exhibited nearly identical uptake efficiency as native Ypep (Figure 4.2B). However, Thr7Lys, Thr7Ser, and Thr7Asn mutants all showed significantly decreased uptake efficiencies. In contrast, the Thr7Phe mutant was significantly improved, and was able to deliver ~7.6-fold more GFP to PC-3 cells, compared to native Ypep. Based on this finding, we produced more mutants containing aromatic residues at residue 7 and assessed their uptake potential. While both Thr7Tyr and Thr7Trp mutants significantly outperformed native Ypep, delivering ~6.8 and ~7.1-fold more GFP, respectively, neither outperformed the Thr7Phe mutant. In contrast, the Thr7His mutant showed

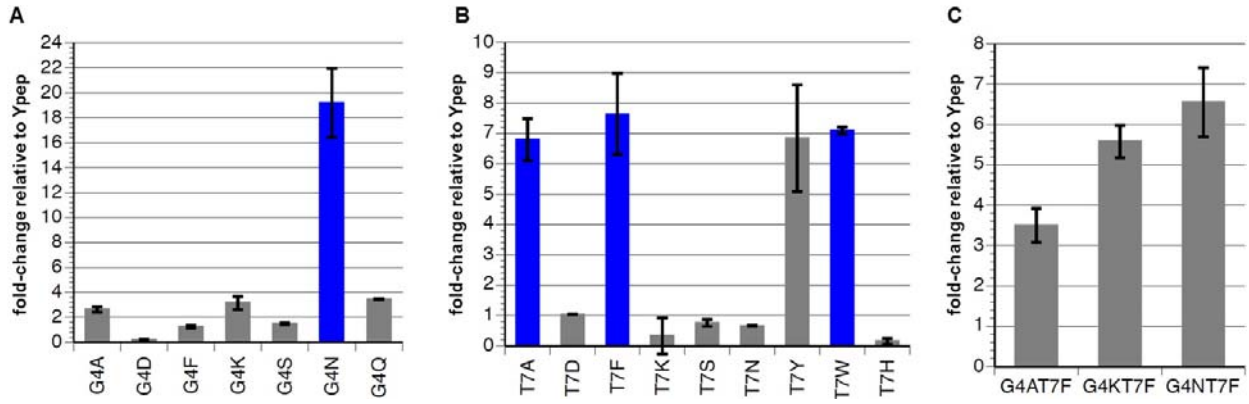

Figure 4.2 Additional mutations to improve Ypep transduction. (A) Fold-change in GFP uptake for Ypep-GFP mutants at residue 4, relative to Ypep-GFP. (B) Fold-change in GFP uptake for Ypep-GFP mutants at residue 7, relative to Ypep-GFP. (C) Fold-change of GFP uptake for Ypep-GFP double mutants at residues 4 and 7, relative to Ypep-GFP. (A-C) In all samples, PC-3 cells were treated with 5 μM solutions of mutant Ypep-GFP, then washed to remove cell surface-bound protein. GFP internalization was measured by flow cytometry. Values and error bars represent the mean and standard deviation of three independent experiments. Blue bars represent the four most active mutants.

significantly lower cell uptake compared to Thr7Tyr and Thr7Trp mutants, as well as native Ypep. Taken together, the reduced transduction we observed for the Thr7His

and Thr7Lys mutants suggests that residues with positive charge, or partial positive charge may not be tolerated at this position.

We next evaluated whether or not the presence of the best mutants at both positions 4 and 7 would enhance uptake efficiency beyond levels demonstrated by the single mutants. Combined synergistic effects can play important roles in many biological processes and macromolecule-substrate interactions.[6] To assess if combinations of beneficial mutants are synergistic, we prepared three Ypep double mutants that containing various combinations of mutations at residues 4 and 7. Ypep double mutants were expressed as N-terminal fusions to GFP and added to PC-3 cells as previously described. Interestingly, uptake efficiencies for these double mutants did not surpass, or match in some cases, the efficiencies of some single mutations. The Gly4Ala:Thr7Phe, Gly4Lys:Thr7Phe, and Gly4Asn:Thr7Phe double mutants were found to be ~3.5, ~5.6, and ~6.5-fold more efficient at GFP transduction than Ypep-GFP, respectively (Figure 4.2C).

4.4 Ypep Mutants are Not Cytotoxic and are Internalized via Energy-dependent Endocytosis

Cytotoxicity of the mutants with the greatest increased uptake effects (Gly4Asn, Thr7Phe, Thr7Trp, and Thr7Ala mutants) were then assessed using 3-(4,5-dimethylthiazol-2-yl)-2,5-diphenyltetrazolium bromide assay (MTT) on PC-3 cells after three hour incubation with 5 μM solutions of Ypep(mutant)-GFP. Results from the assays indicated no apparent cytotoxicity to PC-3 cells for any of the Ypep mutants (Figure 4.3A). GFP uptake was additionally confirmed for these four mutants by live-

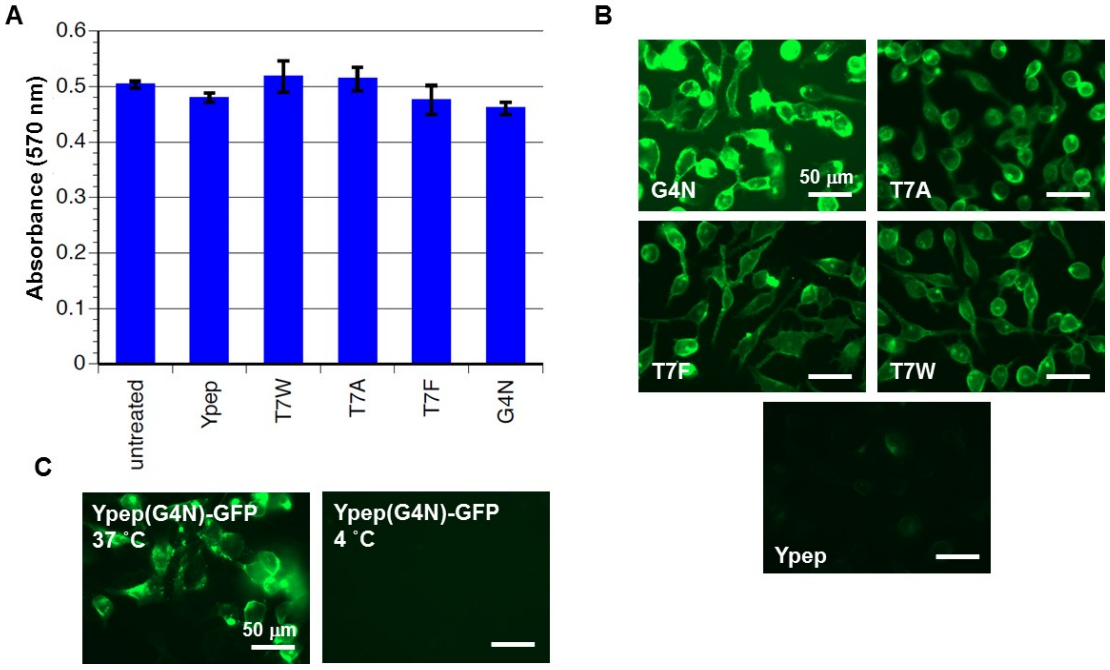

Figure 4.3 Cytotoxicity and mechanism of transduction for Ypep mutants. (A) MTT cell viability assay data. (B) Live cell fluorescence microscopy images of PC-3 cells following treatment with 5 μM solutions of the most efficient mutant Ypep-GFP fusions, then washed to remove cell surface-bound protein. (C) Cell penetration of Ypep(G4N)-GFP at 37 °C or 4 °C. Live cell fluorescence microscopy of images of PC-3 cells following incubation with 5 μM Ypep(G4N)-GFP fusions for 30 minutes at 37 °C or 4 °C. For all microscopy images lamp intensity was set at 50% with a 500 msec exposure.

cell fluorescence microscopy. Images of PC-3 cells treated with 5 μM solutions of the Ypep(Mut)-GFP showed much larger amounts of GFP internalization than cells treated with an equal amount of Ypep-GFP (Figure 4.3B).

We were also interested in learning more about the mechanism of entry for these Ypep-mutants. It was previously shown that the native Ypep-GFP protein entered cells through an energy-dependent endocytotic pathway[1]. Similar studies were connected with the most potent mutant, Ypep(G4N)-GFP to determine if mechanism of entry had been conserved. PC-3 cells were incubated with 1 μM Ypep(G4N)-GFP for three hours at 37 °C or 4 °C. Cells were then extensively washed and GFP uptake measured through flow cytometry and fluorescence microscopy. It was observed that, like the native Ypep-GFP fusion protein, internalization appeared to be inhibited at 4 °C while fluorescence was observed in the cells incubated at 37 °C (Figure 4.3C). These data indicate that the mutant Ypep(G4N)-GFP also enters cells through an energy-dependent endocytic pathway.

4.5 Ypep Mutants Have Greater Transduction Efficiency

Commercially available cell-penetrating peptides such as Tat and penetratin (Pen) have been extensively studied and are often utilized as the main examples within the field[4,7–9]. As previously performed with Ypep-GFP, the uptake efficiency of the four best Ypep mutants were also compared penetratin and Tat. PC-3 cells were incubated

with 1 μM solutions of the four Ypep-GFP mutants, penetratin-GFP, or Tat-GFP for three hours at 37 °C and 5% CO_2. Cells were then washed as previously described and GFP uptake quantified through flow cytometry. Compared to Tat-GFP, all four Ypep mutants facilitated far greater uptake of protein, but only Ypep(G4N)-GFP outperformed delivery by penetratin-GFP at ~23-fold greater fluorescence.

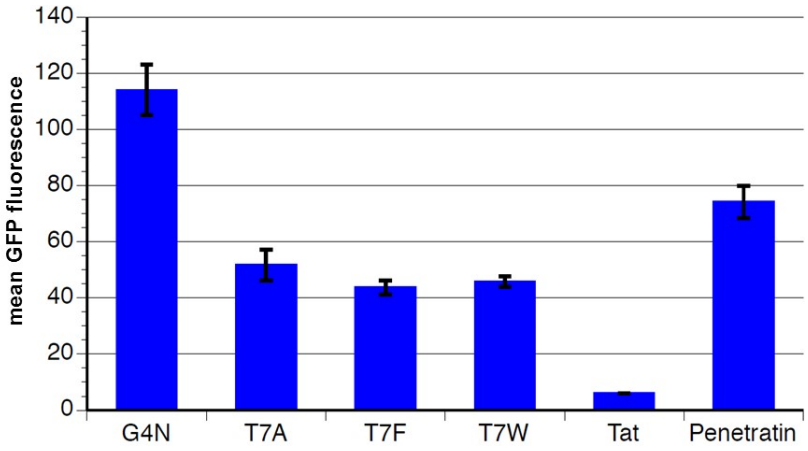

Figure 4.4 Flow cytometry data comparing Ypep(Mut)-GFP, Tat-GFP, or penetrate-GFP delivery to PC-3 prostate cancer cells.. Values and error bars represent the mean and standard deviation of three independent experiments.

4.6 Mutations also Increase the Cell-selectivity of Protein Delivery

Previously, we showed that Ypep-GFP demonstrated only modest specificity for PC-3 prostate cancer cells. We were interested in investigating the effect of the mutations on cell-selectivity. To do so, target PC-3 prostate cancer cells and off-target HEK-293T human embryonic kidney cells were treated with 0.1-1 μM Ypep-GFP or Ypep(Mut)-GFP fusions. Cells were then washed as previously described and GFP internalization quantified through flow cytometry. Similar to the trend of increased

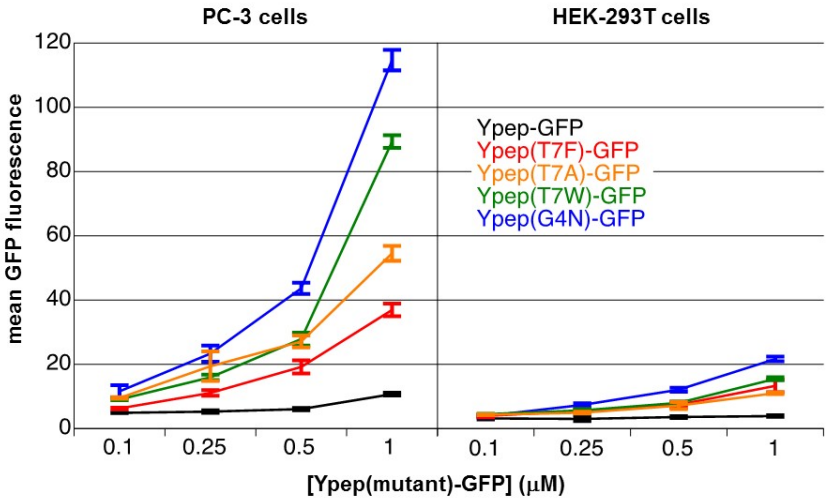

Figure 4.5 Flow cytometry data showing the amount of internalized GFP in PC-3 or HEK-293T cells following treatment with 0.1, 0.25, 0.5, or 1 μM mutant Ypep-GFP, Ypep(T7A)-GFP, Ypep(T7W)-GFP, or Ypep(G4N)-GFP, then washed to remove cell surface-bound protein. Values and error bars represent the mean and standard deviation of three independent experiments.

transduction efficiency demonstrated by each of the mutant Ypep-GFP fusions, they also displayed increased selectivity for PC-3 cells. Consistent with our previous findings, Ypep delivered ~1.6, ~1.8, ~1.7, or ~2.8-fold more GFP to PC-3 cells compared to HEK-293 cells, following treatment with 0.1, 0.25, 0.5, or 1 μM solutions, respectively. While the Thr7Phe mutant exhibited similar selectivity for PC-3 cells (~1.6, ~2.0, ~2.6, and ~2.8-fold following 0.1-1 μM treatment), the Gly4Asn, Thr7Trp, and Thr7Ala mutants were significantly more selective for PC-3 cells. For example, Gly4Asn, Thr7Trp, and Thr7Ala Ypep mutants were ~5.3, ~5.8, and ~5.0-fold more selective for PC-3 prostate cancer cells than for HEK-293T cells. Taken together, these studies indicate a significant improvement in selectivity in conjunction with the transduction efficiency into PC-3 cells.

4.7 Ypep Mutants Can Deliver Functional Enzymes to PC-3 Cells

We've shown that Ypep and the Ypep mutants are capable of delivering a fluorescent protein to the interior of a cell, but in order for a CPP to be successfully utilized in biomedical applications, it needs to be capable of intracellular delivery of a functional enzyme. Luciferase is a class of enzymes that oxidize a photon-emitting substrate, resulting in bioluminescence. These enzymes are used extensively as reporters and cell imaging reagents.[10] NanoLuc luciferase (nLuc) is a recently reported variant of the small luciferase subunit from the deep sea shrimp *Oplophorus gracilirostris*.[11] In order to test of Ypep and its variants were capable of delivering a functional enzyme, we prepared Ypep- and Ypep(G4N)-nLuc fusion proteins. PC-3 prostate cancer cells were treated with 1 μM nLuc, Ypep-nLuc, or Ypep(G4N)-nLuc, washed extensively to remove cell-surface bound protein, treated with furmazine, and luciferase activity measured via bioluminescence. Consistent with the overwhelming majority of proteins, appreciable amounts of nLuc do not penetrate mammalian cells. (Figure 4.6). Similar to our previous findings, relatively modest functional enzyme delivery was achieved via Ypep-dependent delivery. Cells treated with Ypep-nLucwere ~6.1-fold more luminescent than cells treated with nLuc alone (Figure 4.6). In contrast, cells similarly treated with Ypep(G4N)-nLuc were ~41.6-fold more luminescent than cells treated with nLuc alone. These data suggest that Ypep and its mutants are capable of delivering functional enzymes to the interior of PC-3 cells.

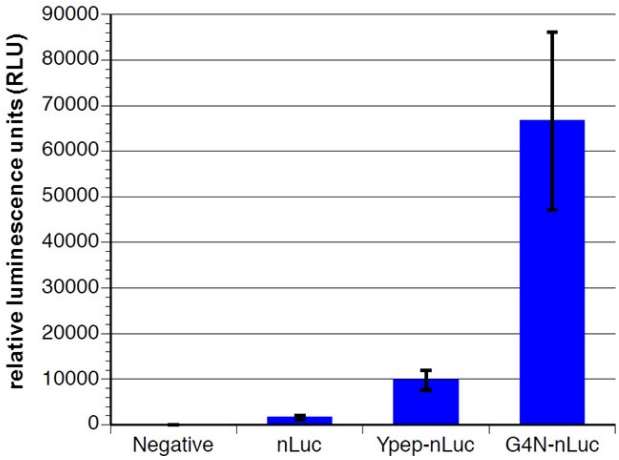

Figure 4.6 Efficiency of nanoluciferase (nLuc) delivery to human prostate cancer cells (PC-3). PC-3 cells were treated with either nLuc, Ypep-nLuc or Ypep(G4N)-nLuc, then washed to remove cell surface-bound protein. Functional nLuc and Ypep-nLuc does not appreciably penetrate PC-3 cells; however, relatively high levels of internalized functional nLuc are observed in cells following treatment with Ypep(G4N)-nLuc.

Importantly, cells were not lysed at any point during the luciferase assay. Therefore, luminescence generated during these experiments is the action of active nLuc enzyme within the cell interior.

4.8 Conclusions

Previously, we had developed a CPP with modest transduction efficiency and cell-selectivity for PC-3 prostate cancer cells. Mutational studies were performed on Ypep, resulting in various constructs with improved selectivity and transduction. In addition to this, we showed that one of these mutants, Ypep(G4N), was capable of delivering functional nanoluciferase to PC-3 cells where the native Ypep was not fully successful. Given this data, it is suggested that the Ypep mutants studied have the

potential to serve as cell selective, cell-penetrating delivery vehicles to PC-3 prostate cancer cells.

4.9 Experimental Methods

Materials

Phosphate buffered saline (PBS) - Hyclone/Thermo Scientific
0.25% Trypsin - Hyclone/Thermo Scientific
Brilliant Blue R-250 - J.T.Baker
Bovin serum albumin - Sigma Aldrich
Fetal bovin serum (FBS) - PAA Laboratories
Triton X-100 - Fisher Scientific
Dulbecco's modified Eagle medium (DMEM) - Hyclone/Thermo Scientific
F-12K Nutrient Mixture (Kaighn's Mod.) - Cellgro/Corning
RPMI-1640 media - Hyclone/Thermo Scientific
Mammalian cell culture dishes - Fisher Scientific
B-PER Bacterial Protein Extraction Reagent - Thermo Scientific
Imidazole - Sigma Aldrich
Modified Lowry Protein Assay Kit - Pierce/Thermo Scientific
Nano-Glo® Luciferase Assay - Promega
TACS MTT reagent- Trevigen
PageRuler Prestained Protein Ladder - Thermo Scientific

Instrumentation

All flow cytometry data was carried out on a MoFlo Flow Cytometer and High Speed Cell Sorter with a solid state iCyt 488nm laser. Relative luciferase units were measured on a Synergy Mx Microplate Reader from BioTek. MTT assay absorbance was measured on Synergy Mx Microplate Reader from BioTek. Fluorescence microscopy images were taken with EVOS FL from Advanced Microscopy Group.

Mammalian cell culture Human prostate adenocarcinoma cells (PC-3) cells were cultured in F12K with 10% Fetal Bovine Serum (FBS) and HEK293T cells cultured in high glucose Dulbecco's 101 modified Eagle medium (DMEM) with 10% Fetal Bovine Serum (FBS). All cells were incubated at 37 °C with 5% CO_2 environment. All cells were obtained from ATCC.

Cloning

All plasmids were constructed on a pETDuet-1 backbone. All peptides and GGS linkers on the N-terminus and C-terminus of sfGFP were assembled from a set of overlapping oligonucleotides. The peptides were then amplified with the sfGFP or nLuc proteins and the plasmids were ligated into *Nco*I and *Kpn*I restriction enzyme cleavage sites in the pETDuet-1 plasmid.

Protein purification

Cells were grown in 500 mL LB cultures at 37 °C to OD_{600} ~0.6 and induced with 1 mM IPTG at 30 °C overnight. Cells were then collected by centrifugation and stored at -20 °C. Frozen pellets were thawed and 20 mL B-PER was added to lyse cells. The lysate was cleared by centrifugation (17000 rpm, 30 minutes) and the supernatant was mixed with 1 mL of Ni-NTA agarose resin for 1 hour. The resin was collected by centrifugation (4950 rpm, 10 minutes). The resin was washed with 50 mL of PBS with 300 mM NaCl and 20 mM imidazole. The protein was then eluted with 5 mL PBS containing 300 mM NaCl and 500 mM imidazole. The proteins were dialyzed against PBS and analyzed for

purity by SDS-PAGE staining with Coomassie Blue. The proteins were then quantified using a modified Lowry protein assay kit. Nanoluciferase (nLuc) proteins were purified in the sample way, except washed with Tris buffers (25 mM Tris-HCl, 100 mM NaCl, pH 8.0) instead of phosphate buffers.

Flow cytometry analysis

Mammalian cells were grown to 90% confluency in a 12-well plate. Cells were then washed once with PBS and 500 μL of diluted protein in PBS was added. The cells were incubated with the protein solution for 3 hours at 37 °C, 5 % CO_2 environment. After the incubation period, cells were then washed once with PBS and two times with PBS·HS (heparin sulfate 20 U/mL) for 10 minutes at 37 °C, 5% CO_2. The cells were then removed from dish with 0.5 mL of 0.25% Trypsin and collected by centrifugation. The cells were then resuspended in PBS-HS and analyzed by flow cytometry.

Live cell fluorescence microscopy

Mammalian cells were grown to 90% confluency in a 12-well plate. Cells were then washed once with PBS and 500 μL of 5 μM protein in PBS was added. The cells were incubated with the protein solution for 3 hours at 37 °C, 5% CO_2 environment. After the incubation period, cells were then washed once with PBS and three times with PBS-HS (heparan sulfate 20 U/mL) for 10 minutes at 37 °C, 5% CO_2. The cells were then imaged on the EVOS FL fluorescence microscope. For 4 ˚C experiments, the PC-3 cells were

incubated at 4 ˚C for 30 minutes prior to the addition of the diluted protein. The incubation period was carried out at 4 ˚C and washed as described above.

MTT assay

PC-3 cells were grown to 90% confluency in a 12-well plate. Cells were then washed once with PBS and incubated with the protein in PBS for 3 hours at 37 °C, 5% CO_2. The solution was removed and the cells were washed twice with PBS-HS (heparan sulfate 20 U/mL). The cells were then incubated with 0.5 mL media with 25 μL of MTT reagent for 4.5 hours. After the incubation, 250 μL detergent was added to the cells and they were incubated for an addition 30 minutes. MTT assay readings were taken with a Synergy Mx microplate reader at 570 nm.

NanoGlo luciferase assay

PC-3 cells were grown to ~80% confluency in a 24-well plate (clear bottom, black well). The nLuc proteins were diluted in TBS (25 mM Tris-HCl, 150 mM NaCl, pH 7.0) and added to the PC-3 cells. Cells were incubated with each solution for 3 hours at 37 ˚C under 5% CO_2 environment. The cells were then washed with TBS, TBS-0.1% tween-20, and TBS-HS (heparan sulfate 20 U/mL). This washing procedure was repeated a total of two times. Then, the cells were incubated with 200 μL TBS and 200 μL Nano-Glo Luciferase Assay Reagent for 10 minutes. Luminescence was measured on a Synergy Mx microplate reader.

Sequence information

Ypep-GFP
MGYTFGLKTSFNVQGGSGGSGGSGGSMGGASKGEELFTGVVPILVELDGDVNGHKF
SVRGEGEGDATNGKLTLKFICTTGKLPVPWPTLVTTLTYGVQCFSRYPDHMKQHDFF
KSAMPEGYVQERTISFKDDGTYKTRAEVKFEGDTLVNRIELKGIDFKEDGNILGHKLE
YNFNSHNVYITADKQKNGIKANFKIRHNVEDGSVQLADHYQQNTPIGDGPVLLPDN
HYLSTQSALSKDPNEKRDHMVLLEFVTAARITHGMDELYKHHHHHH
Tat-GFP
MGYGRKKRRQRRRGGSGGSGGSGGSMGGASKGEELFTGVVPILVELDGDVNGHKFS
VRGEGEGDATNGKLTLKFICTTGKLPVPWPTLVTTLTYGVQCFSRYPDHMKQHDFFK
SAMPEGYVQERTISFKDDGTYKTRAEVKFEGDTLVNRIELKGIDFKEDGNILGHKLEY
NFNSHNVYITADKQKNGIKANFKIRHNVEDGSVQLADHYQQNTPIGDGPVLLPDN
HYLSTPSALSKDPNEKRDHMVLLEFVTAAGITHGMDELYKHHHHHH

Pen-GFP
MGRQIKIWFQNRRMKWKKGGSGGSGGSGGSMGGASKGEELFTGVVPILVELDGDV
NGHKFSVRGEGEGDATNGKLTLKFICTTGKLPVPWPTLVTTLTYGVQCFSRYPDHMK
QHDFFKSAMPEGYVQERTISFKDDGTYKTRAEVKFEGDTLVNRIELKGIDFKEDGNIL
GHKLEYNFNSHNVYITADKQKNGIKANFKIRHNVEDGSVQLADHYQQNTPIGDGP
VLLPDNHYLSTQSALSKDPNEKRDHMVLLEFVTAAGITHGMDELYKHHHHHH

nLuc
MVFTLEDFVGDWRQTAGYNLDQVLEQGGVSSLFQNLGVSVTPIQRIVLSGENGLKID
IHVIIPYEGLSGDQMGQIEKIFKVVYPVDDHHFKVILHYGTLVIDGVTPNMIDYFGRPY
EGIAVFDGKKITVTGTLWNGNKIIDERLINPDGSLLFRVTINGVTGWRLCERILAHHH
HHH

Ypep-nLuc
YTFGLKTSFNVQGGSALALGMVFTLEDFVGDWRQTAGYNLDQVLEQGGVSSLFQNL
GVSVTPIQRIVLSGENGLKIDIHVIIPYEGLSGDQMGQIEKIFKVVYPVDDHHFKVILHY
GTLVIDGVTPNMIDYFGRPYEGIAVFDGKKITVTGTLWNGNKIIDERLINPDGSLLFRV
TINGVTGWRLCERILAHHHHHH

REFERENCES

(1) Deporter, S. M., Lui, I., Mohan, U., and Mcnaughton, B. R. (2013) Resource A Protein Transduction Domain with Cell Uptake and Selectivity Profiles that Are Controlled by Multivalency Effects 434–444.

(2) Madani, F., Lindberg, S., Langel, U., Futaki, S., and Gräslund, A. (2011) Mechanisms of cellular uptake of cell-penetrating peptides. *J. Biophys. 2011*, 414729–414739.

(3) Rothbard, J. B., Kreider, E., VanDeusen, C. L., Wright, L., Wylie, B. L., and Wender, P. a. (2002) Arginine-rich molecular transporters for drug delivery: Role of backbone spacing in cellular uptake. *J. Med. Chem. 45*, 3612–3618.

(4) Vives, E. (2003) Cellular utake of the Tat peptide : an endocytosis mechanism following ionic interactions AN IMPROVED DELIVERY UPON 265–271.

(5) Derossi, D., Chassaing, G., and Prochiantz, A. (1998) Trojan peptides: the penetratin system for intracellular delivery. *Trends Cell Biol. 8*, 84–87.

(6) Mammen, M., Choi, S.-K., and Whitesides, G. M. (1998) Polyvalent Interactions in Biological Systems: Implications for Design and Use of Multivalent Ligands and Inhibitors. *Angew. Chemie Int. Ed. 37*, 2754–2794.

(7) Wadia, J. S., Stan, R. V, and Dowdy, S. F. (2004) Transducible TAT-HA fusogenic peptide enhances escape of TAT-fusion proteins after lipid raft macropinocytosis. *Nat. Med. 10*, 310–315.

(8) Cronican, J. J., Thompson, D. B., Beier, K. T., McNaughton, B. R., Cepko, C. L., and Liu, D. R. (2010) Potent delivery of functional proteins into Mammalian cells in vitro and in vivo using a supercharged protein. *ACS Chem. Biol. 5*, 747–52.

(9) Thorén, E. G., Persson, D., Karlsson, M., and Nordén, B. (2000) The Antennapedia peptide penetratin translocates across lipid bilayers - the first direct observation. *FEBS Lett. 482*, 265–268.

(10) Thorne, N., Inglese, J., and Auld, D. S. (2010) Illuminating insights into firefly luciferase and other bioluminescent reporters used in chemical biology. *Chem. Biol. 17*, 646–57.

(11) Hall, M. P., Unch, J., Binkowski, B. F., Valley, M. P., Butler, B. L., Wood, M. G., Otto, P., Zimmerman, K., Vidugiris, G., Machleidt, T., Robers, M. B., Benink, H. A., Eggers, C. T., Slater, M. R., Meisenheimer, P. L., Klaubert, D. H., Fan, F., Encell, L. P., and Wood, K. V. (2012) Engineered luciferase reporter from a deep sea shrimp utilizing a novel imidazopyrazinone substrate. *ACS Chem. Biol. 7*, 1848–57.